EPOXY COMPOSITE UNDER FATIGUE LOADING: ACOUSTIC EMISSION STUDIES

by

NARENDRA KUMAR ARYA

DEPARTMENT OF AEROSPACE ENGINEERING

INDIAN INSTITUTE OF TECHNOLOGY KANPUR

APRIL 1990

DAMAGE GROWTH IN CARBON FABRIC REINFORCED EPOXY COMPOSITE UNDER FATIGUE LOADING : ACOUSTIC EMISSION STUDIES

A Thesis Submitted
in Partial Fulfillment of the
Requirements for the Degree of

MASTER OF TECHNOLOGY

by

NARENDRA KUMAR ARYA

to the

DEPARTMENT OF AEROSPACE ENGINEERING INDIAN INSTITUTE OF TECHNOLOGY, KANPUR
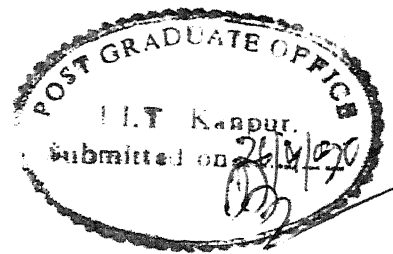
APRIL, 1990

AE-1990-M-ARY-DAM
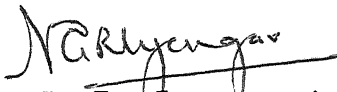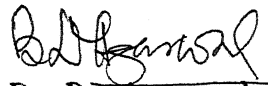
CERTIFICATE

This is to certify that the thesis entitled, "DAMAGE GROWTH IN CARBON FABRIC REINFORCED EPOXY COMPOSITE UNDER FATIGUE LOADING : ACOUSTIC EMISSION STUDIES", by Narendra Kumar arya is a record of the work carried out under our supervision and has not been submitted elsewhere for a degree.

(N. G. R. Iyengar)
Professor
Aerospace Engineering Department
Indian Institute of Technology
Kanpur - 208 016

(B. D. Agarwal)
Professor
Mechanical Engineering Department
Indian Institute of Technology
Kanpur - 208 016

April, 1990

ACKNOWLEDGMENTS

CONTENTS

LIST OF FIGURES

LIST OF TABLES

ABSTRACT

Fatigue behaviour of carbon fabric reinforced epoxy composites has been studied. Emphasis has been placed on the study of damage growth during fatigue loading. Initially damage growth was studied on the basis of fatigue modulus and was observed that in carbon epoxy composite, like kevlar epoxy composite, the damage growth occurs in three stages. Beginning of the third stage of damage represents a critical condition beyond which damage grows very fast and failure occurs. The third stage of damage usually spans over last 4 or 5% of total fatigue life.

Further studies on damage growth have been carried out using acoustic emission technique. As a first step in employing this technique for damage identification and monitoring, acoustic emission characteristics of internal damage mechanisms (that is fibre breaks, matrix cracks, and delamination) have been determined. It is accomplished by conducting tests on specimens in which only one type of damage is predominant in a single test. The results indicate that fibre breaks, matrix cracks, and delamination cracks can be identified on the basis of event duration (ED).

To study damage growth during a normal fatigue test, recorded acoustic emission events were first classified into the three categories representing three damage mechanisms indicated above. The results indicate that neither the number of damage events causing acoustic emissions nor the energy associated with them correlates with the damage indicated by fatigue modulus.

CHAPTER 1

INTRODUCTION

1.1 COMPOSITE MATERIALS :

Composites are materials consisting of one or more discontinuous phases embedded in a continuous phase. The discontinuous phase is usually harder and stronger than the continuous phase and is called the reinforcement or reinforcing material, whereas the continuous phase is termed the matrix. The two phases are chemically distinct on a macroscale and have a distinct interface separating them. However they act in concert.

Composite materials are well known for their light weight, high strength, and high stiffness properties. Additional advantages that the composites offer over the conventional materials include flexibility in design, ease of fabrication, corrosion resistance, etc. Carbon fibre reinforced epoxy composites are one of the most widely used composite materials for aerospace applications. They have high specific tensile strength, compressive strength and stiffness.

1.2 FATIGUE BEHAVIOUR OF COMPOSITE MATERIALS:

It is well known that, when materials are subjected to repeated fluctuating or alternating loads, they may fail even though the maximum stress may never reach the ultimate static strength of the material. In other words the fatigue strength of a material is lower than its static strength. This is true of all existing materials including metals, plastics and composite materials. However fatigue behaviour of composite materials is

quite different from that of isotropic materials such as metals and polymers. Fatigue in metals is understood in terms of nucleation and growth of a single dominant flaw, whereas fatigue in composites is characterized by initiation and growth of multiple cracks. Because of the heterogeneity inherent in composites, cracks in composites do not have the implications as those in metals. Damage in composites can be any one or several of the following forms: fibre breaks, matrix cracks, interfacial debonds and delamination between plies of laminate. Many of these damage mechanisms occur long before the ultimate failure, and hence, there can be many types of subcritical failures. The damage mechanism of composite materials should be clearly understood and assessed, if properties of these materials are to be improved and engineering designs using these materials are to be more economical and reliable.

Fatigue of composites has been very widely investigated since the early days of their use in structural applications. It was recognised nearly 20 years ago that the fatigue damage in composites is progressive (1-4). The internal material damage results in the reduction in strength and stiffness. The residual strength and stiffness are influenced by such factors as fibre volume fraction, type of matrix, interface properties, frequency, environment, ply orientation and stacking sequence, etc. In recent years, a lot of effort is being directed towards identification and characterization of fatigue damage and its influence on residual properties using non-destructive evalution methods such as acoustic emission and ultrasonics (5-26). Harris and associates (5-9) have extensively used acoustic emmision

technique to study static and fatigue behaviour of reinforced plastics. Ansell (10) investigated acoustic emmision from softwood in tension. Curtis and Moore (11) monitored damage development by optical microscopy, ultrasonic C-scanning, video recording and infra-red thermography to compare the fatigue performance of woven and non-woven CFRP laminates. Amijima and associates (12-15) studied the fatigue behaviour of different types of composites subjected to random loading. Ohlson (17) studied damage in biaxial fatigue of composites. Benzeggagh et al (18) analysed mode-I delamination testing using acoustic emmission. Davidson (19) demonstrated the utility of the stereoimaging technique in the study of composite materials. Reynolds (20-21) has suggested the use of nondestructive methods to study glass fibre reinforced composites. Wevers et al (22) analyzed fatigue damage of Carbon Fiber Reinforced Epoxy composites by means of acoustic emmission. Echalier and Falchi (23) studied mechanical behaviour and acoustic emission of wound structures under static and fatigue loading. Bader and Boniface (24) followed the progress of damage during quasi-static and cyclic loading in GFRP and CFRP laminates by acoustic emission, optical microscopy and penetrant enhanced X-radiography. Valentin and Bunsell (25) monitored damage accumulation by A.E. technique in crossplied CFRP to discriminate between the different mechanisms of fracture in composites by amplitude analysis of the recorded signals. They found that even in a unidirectional CFRP, the main mechanism of degradation fibre-breakage coexists with secondry phenomenon such as matrix cracking or interface failure. American Society for Testing and Materials organized a symposium

on "Damage in Compossite Materials: Basic Mechanisms, Accumulation, Tolerance and Characterization" where different aspects of the subject were discussed. Several useful papers are contained in the proceedinds (26). Agarwal and Majumdar (27) monitored dmage accumulation of Kevlar fabric reinforced epoxy composite under axial fatigue loading. They found that fatigue modulus, which decreases continuously with number of cycles, is an adequate parameter to represent fatigue damage. Fatigue damage occurs in three stages, namely initiation, steady, and propagation stages. This damage behaviour can be represented by an empirical equation with constants determined experimentally. The beginning of damage propagation stage appears to represent a critical condition similar to the appearance of a crack during fatigue of metals.

1.3 SCOPE OF PRESENT WORK :

The present work has been carried out on carbon fabric reinforced epoxy composite laminates. Method of fabrication, specimen preparation and testing details are given in chapter 2. Acoustic emission data recording and analysis is described in chapter 3. Static behaviour, fatigue life and damage based on fatigue modulus are discussed in sections 4.1, 4.2 and 4.3 respectively. Acoustic emission characteristics of internal damage mechanisms are discussed in section 4.4. Damage growth has been studied through acoustic emissions (section 4.5). Projecting the highlights of the current investigations, summary, conclusions drawn and suggestions for future work are indicated in chapter 5.

CHAPTER 2

EXPERIMENTAL DETAILS

2.1 PREPARATION OF SPECIMENS :

It was decided to carry out investigations on carbon/epoxy composite and prepare the specimens with carbon fabric of unidirectional weave as reinforcing material. The details regarding material and fabrication are given in sections 2.1.1, 2.1.2 & 2.1.3. Fabrication of specimens used for controlled experiments is given in section 2.1.3

2.1.1 MATERIAL USED :

The material selected for the study was Carbon fabric reinforced epoxy composite. The manufacturer's specifications of Carbon fabric and epoxy resin are given in tables 2.1 & 2.2 respectively. Although fabric material is inferior in fatigue properties than nonwoven material, it is widely used in practical applications due to ease of fabrication. The carbon fabric used, has fiber volume ratio in warp and fill directions as 91:9 (10:1 approximately) which is generally referred to as the unidirectional weave. All The investigations made in the present study are for warp direction. Curing times suggested by the manufacturer are given in table 2.3.

2.1.2 LAMINATE FABRICATION :

Composite laminates were cast in the laboratory by hand lay-up technique. Fabric was cut to a size of 46 x 23 cm^2 so as to obtain a good central portion for specimen preparation. Eight layers of fabric were used in each laminate. About 250 gms. of

TABLE 2.1 : CARBON FABRIC SPECIFICATIONS

Manufacturer	– Brochier Sa
Style	– G 8Ø8
Weight, gm/m^2	– 22Ø
Unidirectional Plain	– % Warp 91
	– % Weft 9
Yarn Composition	– Warp 3 KHR
	– Weft 1 KHR
Width (cm)	– 1ØØ
Thickness (Microns)	– 24Ø
Decomposition Temp.	– 27Ø$^\emptyset$ – 28Ø$^\emptyset$c

TABLE 2.2 : EPOXY SPECIFICATIONS

Product	- Ciba Geigy India Ltd.
Category : Resin	- Araldite LY 556
Hardener-	Hardener HY 951 (10% of Araldite by weight
Viscosity	- 5000 - 8000 cp
Pot Life	- 30 mts to 1 hr.
Specific Gravity	- 1.2 - 1.3
Tensile Strength	- 55 - 130 MPa
Tensile Modulus	- 2800 - 4200 MPa
Poisson's Ratio	- 0.20 - 0.33
Flexural Strength	- 125 MPa
Decomposition Temp.	- 270 - 280 ^{0}c

Table 2.3 : Epoxy Curing Chart

Curing Temp. (^{0}c)	Curing Time
20	14 - 24 hr.
50	5 - 7 hr.
80	1 - 2 hr.
100	15 - 30 min.
140	5 - 10 min.

epoxy resin (Araldite LY556) was preheated to about $100^{\circ}C$ and the temperature maintained for one hour to remove the absorbed moisture. The resin was then allowed to cool to room temperature.

Composite laminates were cast between two 25 mm thick Mild Steel plates. The M.S. plates were nickel coated on one side and affixed with heating element on the other side. A milar sheet was placed on the lower mould plate. The resin and hardener were thoroughly mixed. The amount of hardener was 10% of epoxy used. A layer of resin was spread over the milar sheet and one piece of carbon fabric was placed over it. Resin was applied over the fabric by means of a brush. This process was repeated till all the eight layers of fabric were placed. To enhance wetting and impregnation the resin was tapped and dabbed with spatula before spreading resin over fabric pieces. Another myler sheet was placed over the top most layer. Steel spacers of two mm thickness were placed at all four corners between the two myler sheets. A rubber roller was rolled over the top myler sheet along the weft direction of the fabric to squeeze out excess epoxy. The upper mould plate was then placed in position. The nuts were tightened on the bolts to apply a uniform pressure.

The laminate thus prepared was cured for six hours at room temperature followed by 12 hours curing at $55 - 60^{\circ}C$. The rate of heating could be controlled through a variac.

The volume fraction of fibers in the laminate has been calculated using area density of the fabric as follows.

$$V_f = (A.N.d_{fa} / d_f) / (A.t)$$

$$= (N.d_{fa}) / (d_f.t)$$

where,

V_f : Fiber volume fraction

A : Area of composite laminate

d_{fa} : Area density of the fabric

d_f : Density of the fibers

t : Thickness of the laminate

In the present case we have,

$N = 8$

$d_{fa} = 0.220 \ Kg/m^2$

$d_f = 1.9 \times 10^3 \ Kg/m^3$

$t = 2 \times 10^{-3} \ m$

Hence,

$Vf = 0.4631 \ (46.31\%)$

2.1.3 PREPARATION OF SPECIMENS :

Preparation of test specimens involves cutting the laminates to the desired size, finishing them and fixing end tabs on them.

Rectangular specimens of the dimension, as shown in Fig. 2.1 were cut from fabricated laminates using a circular saw. The width of the specimens was kept as 22 mm because diameter of the acoustic emission sensors is 22 mm. The end tabs were made of glass fabric reinforced epoxy. The tabs were 45 mm long, 22 mm wide and 2 mm thick. The tabs were affixed to the test pieces using epoxy as adhesive. At a time six test pieces were affixed with tabs in a drill press vice and curing was done for 24 Hrs. at room Temperature. To avoid sticking of two tabs of different

specimens, milar sheets were inserted between them. A finally prepared test specimen is shown in fig. 2.2a.

2.1.4 SPECIMEN PREPARATION FOR CONTROLLED EXPERIMENTS:

Three types of controlled experiments were conducted to find out the characteristics of matrix cracks, fiber breaks and delaminations in CFRP specimens. For identification of matrix cracks, specimens were made of unreinforced epoxy (Fig. 2.2b). Required amount of epoxy and hardener in ratio of 10:1 by weight was poured in mould made of perspex sheets to get plates of unreinforced epoxy. Specimens were cut from this plate using circular saw. Scratches were made in the middle portion of the specimens using a knife. For identification of fibre breaks specimens were prepared with only fibers in the middle region (Fig. 2.2c). Procedure of there fabrication was same as described in section 2.1.2 except that epoxy was not put in the middle region. For delamination experiments specimens were prepared with milar sheets inserted between layers (Fig.2.2d).

2.2 EXPERIMENTAL SETUP :

For present investigations, all the tests were carried out on MTS 810 servohydraulic testing system (Fig.2.3). The testing machine has the load range capacity of -100 KN to +100 KN which can be applied in the form of a sine, ramp, haversine, triangular and some other programmable waveforms. Some information about the system is given in section 2.2.1. Acoustic data was recorded using AET 5000 series Microcomputer-Based Acoustic Emission Monitoring System (Fig. 2.4). Some information about the system is given in section 2.2.2. The system is interfaced with a
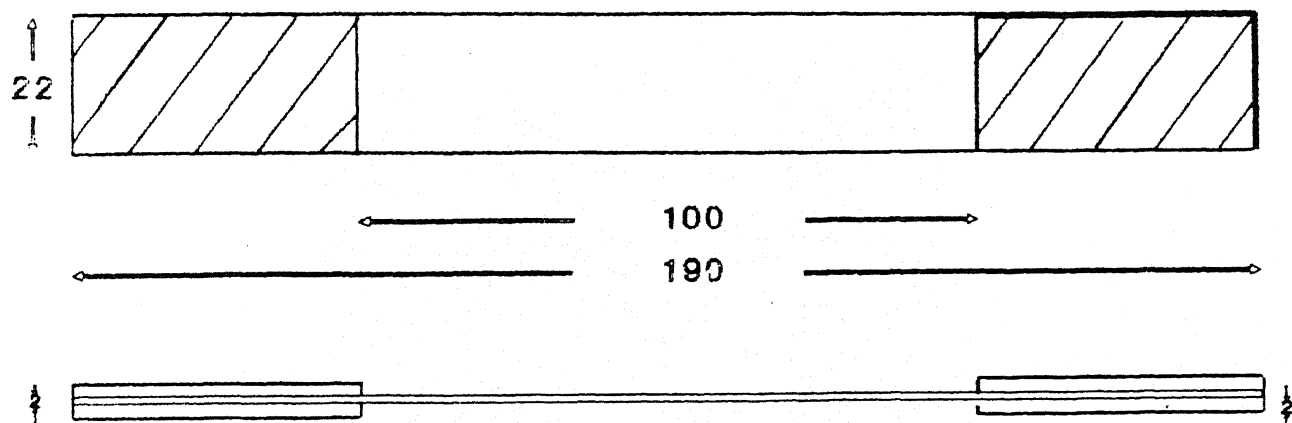
ALL DIMENSIONS IN MM

Fig. 2.1 SPECIMEN GEOMETRY
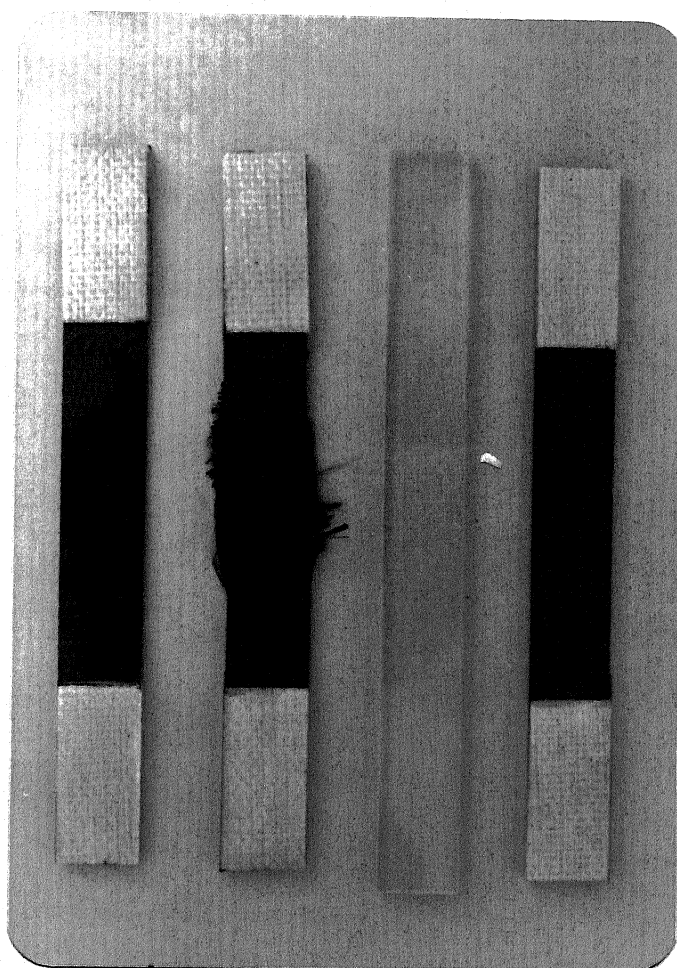
(a)   (b)   (c)   (d)

Fig. 2.2. THE SPECIMENS PREPARED

    (a) CFRP specimen for tensile and fatigue tests

    (b) Specimen with only fibers in middle region

    (c) Specimen made of only resin

    (d) Specimen with miler sheet pieces inserted between layers
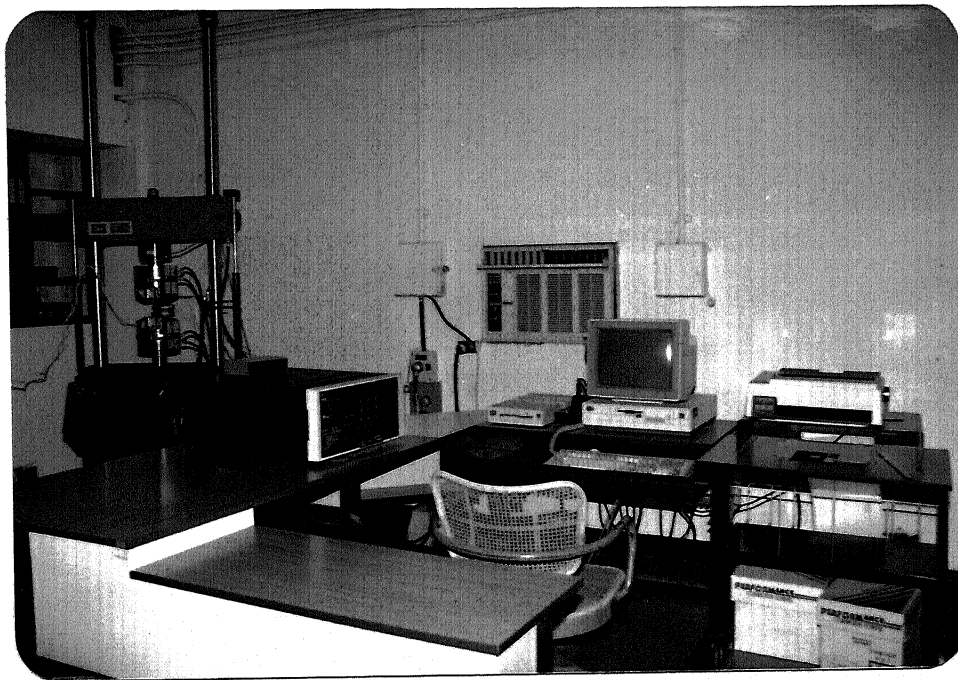
(a)
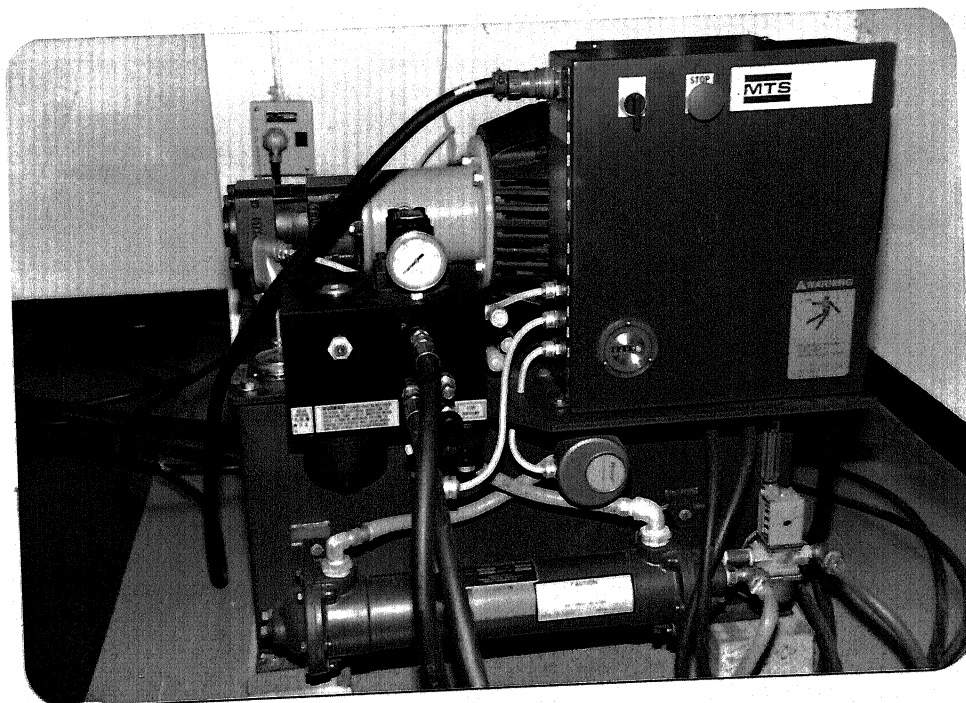
(b)

Fig. 2.3. MTS 810 MATERIAL TESTING SYSTEM

(a) Load Unit, Microconsole and PC

(b) Hydraulic Power Supply

Fig. 2.4. Acoustic Emission Data Monitoring System, its graphics terminal, its plotter and a PC-XT interfaced with it.

PC-XT so that the data can be transferred to soft sectord floppies to be processed with available and developed software.

2.2.1 MATERIAL TESTING SYSTEM

The model 810 Material Testing system is designed to accommodate a wide variety of standard material tests. This uses 458.20 microconsole to provide closed loop control of the servohydraulic system. Specimen is gripped in the load unit. Hydraulic power supply is linked to the microconsole. To control the tests microconsole has a Displacement AC controller, Load DC controller and Strain DC controller. Testing can be done in any of these control modes. To generate a waveform microconsole has a microprofiler which can be operated in three modes viz. programmed, direct and remote. In programmed and direct modes a programme which has been keyed in through a keypad is used to generate a waveform. In remote mode a PC (IBM PS/2) controls the test using 759 test software from MTS corporation. This software programs the microprofiler as well as records the data. This can perform Tensile, Fatigue and some other type of tests. An extensometer is used to record strain.

When this work was started the test system was not operational. The Hydraulic Power Supply was getting switched off after about ten minutes of starting it. After a lot of investigation it was found that the water regulating valve which controls the water going into the heat exchanger was not adjusted to suit Indian conditions. The problem was resolved by setting it properly. After some days HPS again started showing problem. This time it was found to be due to dirt in water filter hence was

overcome by cleaning it. Then there was problem with the test software. It was giving wrong values for stress and it can perform fatigue tests upto a frequency of 1.5 Hz only. Source code is not available with us for this software but MTS has provided another software written in BASIC called TESTLINK which has some some example programs to do the tests. A modified version of TESTLINK was prepared called ARYATEST with which fatigue tests can be performed upto a frequency of 15 Hz. Frequency range was increased by reducing data samples in one cycle from 100 to 10. ARYATEST stores stress and strain data in file which can be used for any kind of analysis. Later on modified version of 759 was also received but this also can perform fatigue tests upto 1.5 Hz frequency only and does not give data in a usable file however this gives right value for stress. After some tests were carried out successfully, another major problem of leak in lift cylinder seals was encountered. The seals were changed without waiting for MTS engineer. There were other problems also like extensometer slipping, problem due to lower range of strain cartridge not being available etc. which were solved in some way or other.

2.2.2 ACOUSTIC EMISSION MONITORING SYSTEM :

The AET 5000B System is microcomputer-based to allow fast data acquisition and multi-test processing. Its a two-to-eight channel system with real time data monitoring capability. The system measures and collects data independently on all active channels for the following event parameters: ring down counts, event duration, peak amplitude, rise time, energy and slope. The

system is housed in an 11" x 17" x 32" enclosure, with a separate intelligent graphics terminal. It has accessories viz. sensors, connectors, cables, preamplifiers, filters and couplant for running an acoustic emission test.

2.3 EXPERIMENTAL PROCEDURE :

While cutting the laminates specimens were numbered. The number included information about material, type of test on the specimen, laminate number and specimen location on the laminate. For example C\F712 corresponds to specimen made of only carbon, laminate number 7, location on laminate 12 th from one end and fatigue test. It was found that tensile strength was different for specimens cut from different laminates. There was small variation in tensile strength of specimens of same laminate also. Hence to get a good estimate of tensile strength of specimens to be tested in fatigue, tensile tests were conducted on at least three specimens cut from each laminate chosen from different locations.

2.3.1 TEST PARAMETERS FOR LOADING :

The stress ratio R (ratio of minimum stress to maximum stress in a fatigue cycle) for all the fatigue tests was 0.1. Generally this value of R is chosen because for this value, load is always tensile and varies in a wide range giving good effect of fatigue. Initially tests were conducted at maximum stress $S_{max} = 0.9 \, S_u$ as well as $S_{max} = 0.85 \, S_u$ at frequencies of 1.5 Hz as well as 10 Hz. Later on, for all tests for which acoustic data was recorded, $S_{max} = 0.9 \, S_u$ and frequency f = 1.5 Hz were selected because so that a fatigue life of around 1000

cycles is obtained and failure is inside the test section. All fatigue tests were condusted in Load control mode.

2.3.2 PARAMETERS FOR ACOUSTIC EMISSION DATA MONITORING

The distance between the two sensors, used in these tests, was divided into 100 segments for the purpose of monitoring the line location. These segments correspond to locations "0" to "100".

The preamplifier gain for both the sensors was set to a value of 60 dB. (Since the preamplifiers used with each of the sensors have a gain equal to this value). The threshold level was set at a value of 1 volt fixed since the machine noise through grips and other noise level was observed to be less than this value after mounting the specimen. The type of test conducted was linear, with sensor numbers 1 and 2 having locations of "0" and "100" respectively. Maximum DT (delay time) was initially set as 0 which gets automatically corrected to a value obtained during the course of calibration.

Ranges of different acoustic emission parameters were set to their default values itself and are shown in Table 2.4. These ranges are used as a basis for discrimination of selected and rejected events.

2.3.3 CONDUCTING THE TESTS

The specimen surfaces were cleaned with acetone and made dirt free. Two sensors were then attached to the specimen surface with centers 6 cm apart and equi-distant from the centre. The sensors were attached with a couplant, SC6 silicon grease smeared on the shoe of the sensor in a thin layer.

TABLE 2.4 : RANGES OF AE PARAMETERS.

	MIN	MAX
Event Duration	Ø	6552Ø
Ring Down Counts	Ø	4Ø96
Rise Time	Ø	6452Ø
Peak Amplitude	Ø	117
Slope	Ø	6552Ø
Energy	Ø	165
Analog Parameters (# 1/2/3)	Ø	1Ø23Ø

Cellophane tape was wrapped around the sensors and the specimen for intimate contact between the sensor shoe and the specimen.

Firstly the calibration for the test is performed on the specimen to get a representative speed of sound in the specimen material. Calibration is performed by placing a standard acoustic emission source (another sensor which is connected to the mainframe's 5 volt output pulse) very close to one of the sensors outside the 100 segment region. The AE source simulator sends out a signal at a constant level. This signal is picked up by the two sensors, and the difference in arrival time of these two signals is used by the system computer to determine the speed of sound in the specimen. The pulser is then removed from the specimen.

Cartridges of proper ranges of load, displacement and strain are inserted in MTS microconsole. Microprofiler is put in remote mode and run enable function is selected. Test program is run on the PC and details regarding units, specimen identity, control mode, maximum load level, minimum load level, frequency, load range, stroke range, strain range, failure threshold, specimen geometry, specimen width, specimen thickness,etc. are entered. Transducer output for load is set to zero using zero control and DC error is set to zero using set point. Hydraulic power supply is switched on and actuator is moved up using set point as per requirement. Specimen is then mounted in the hydraulically operated grips of load unit (Fig.2.5). Transducer outputs for load, strain and displacement are set to zero and interlocks are switched on before starting the test. Test is then started by entering START in PC.
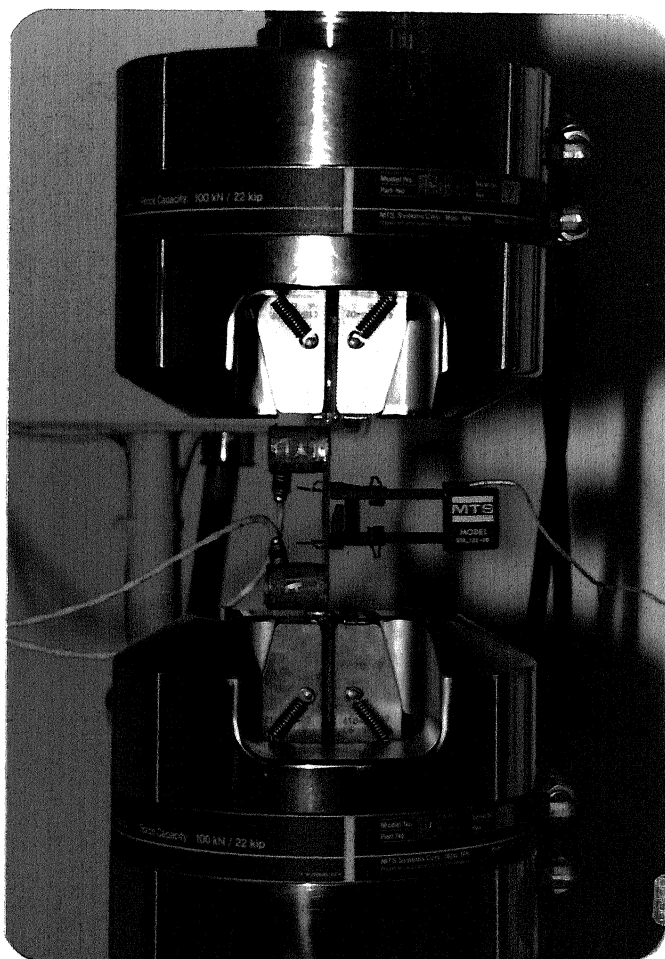
Fig. 2.5. Specimen with acoustic sensors and extensometer
mounted in grips

CHAPTER 3

ACOUSTIC EMISSION DATA RECORDING AND ANALYSIS

3.1 INTRODUCTION

Acoustic emission is a transient elastic wave generated by the rapid release of energy within the material. AE technology and its application focus on events that cause energy release in a material. AE technique detects these internal energy releases using transducers. Monitoring of these events permits detection and location of flaws as well as prediction of impending failure.

Advantages of AE testing lie in its abilities of real time evaluation, continuous monitoring, detection of active defects, source location and its high sensitivity. Moreover it does not interfere with the loading. Limitations of AE testing are due to difficulties in discriminating between signals emanating from different types of damage mechanisms.

3.2 ACOUSTIC EMISSION TERMINOLOGY :

A typical acoustic emission signal, shown in Fig. 3.1 illustrates various terms used as measures of AE activites viz ringdown counts, peak amplitude, energy, event duration, rise time and slope. These terms along with some other terms associated with acoustic emission technique are defined below.

Threshold Voltage : This is the minimum voltage, an acoustic emission signal must posses to be declared a valid event. This is used to separate noise from the useful acoustic signals.
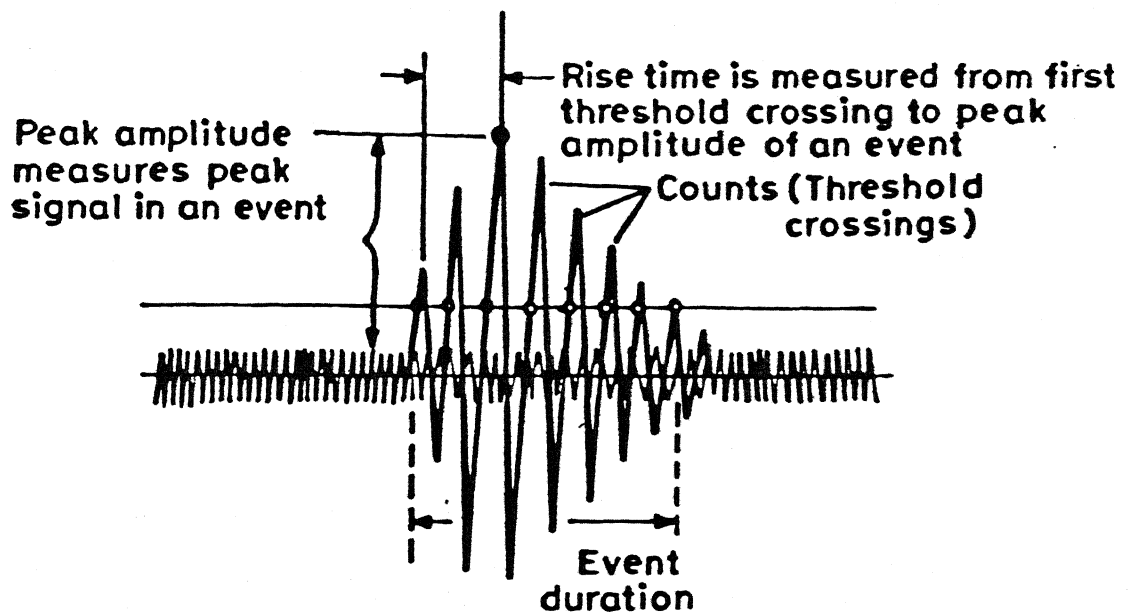
Fig. 3.1 Characterization of burst emissions by the thershold method.

Acoustic Emission Event : It is a signal detected by the transducer with amplitude larger than the preset threshold and originating from a single source or damage event. An event is said to have begun when the AE signal amplitude exceeds the preset threshold for the first time and is said to be over when the signal crosses the threshold last time after which the next threshold crossing is not observed within a specified time gap. This specified time gap (the amount of time that the event detector waits to ensure that the event is over) is called "timeout period". For the present work the time out period is 32 micro seconds.

Ring Down Count : The number of times the AE signal amplitude exceeds the threshold value during an AE event is known as ring down count (RDC) of that event.

Peak Amplitude : It is the amplitude of the largest signal in an AE event. This is measured after passing the signal through preamplifiers and given as gain in decibels (db). Relationship between the peak amplitude in milivolts and that in db is given below:

$$PA(\text{in db}) = 20 \log_{10} (PA \text{ in mV})$$

Peak amplitude at sensors can be obtained by dividing this peak amplitude in mV by 1000 since the amplifier gain is 60 db and thus amplify the signal 1000 times.

Event Duration : It is the time interval between the first and the last threshold crossings of signals in an event. This is measured in micro seconds.

Rise Time : It is the time between the start of an AE event and its peak signal. This is also measured in micro seconds.

Slope : It is the time rate of reaching the peak amplitude and is calculated as the peak amplitude divided by the rise time. It is expressed in mV/μs. **Energy** : Since acoustic emission activity is attributed to rapid release of energy in a material, the energy content of the acoustic emission signal can be related to this energy release and can be expressed in several ways.

The equipment used for this work computes energy as-

$$\text{Energy} = 10\ \log_{10}[\ PA^2 * ED/25\ ]$$

where, PA is in mV and ED is in μs.

if PA is taken in db :

$$\text{Energy} = \text{Peak amplitude} + 10\ \log_{10}(\ ED/25\ )$$

Arrival Time Difference : This is the time interval between the instants at which a signal is detected by the two sensors. This can be used to locate the AE source.

3.3 ACOUSTIC EMISSION DATA RECORDING:

In fiber composites various types of internal damages occur during loading. There are three basic types of internal damages viz. fiber breaks, matrix cracks and debonding. Matrix may fail in tension or in shear. When a matrix crack occurs at the interface of two laminae, it is called delamination crack. The fibers may pull out of the matrix material as a result of fiber break and debonding. These internal damage mechanisms are schematically shown in Fig. 3.2.
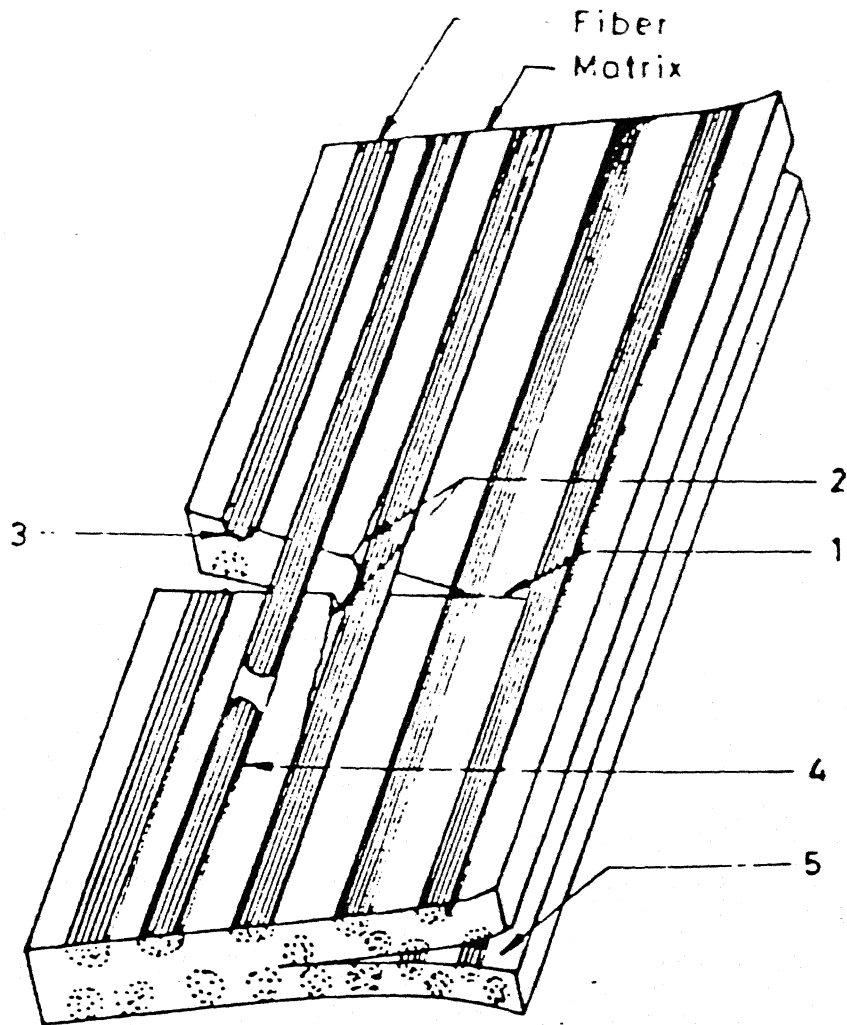
1   Matrix Cracking
2   Fiber – Matrix Debonding
3   Fiber Break
4   Fiber Pull out
5   Delamination

Fig. 3.2 Sources of AE in fiber reinforced composites

Whenever some kind of damage takes place, an acoustic signal is emitted. These acoustic emissions are picked up by sensors mounted on the specimen. The sensor converts the acoustic signal into an electrical signal (voltage difference) which is amplified 1000 times by preamps (i.e., gain 60 db). The gain in db is defined as $Gain(db) = 20 \log_{10} (V_2/V_1)$ where V_1 is the input voltage and V_2 is the out put voltage). The gain of 60 db corresponds to 1000 times magnification of signal voltage. A part of the signal from the sensors is passed to Amplitude/Rise time module (ARM) which measures the peak amplitude (in db) and rise time (in μs) of the signal. It should be noted here that this amplitude of the signal is measured after gain of 60 db at preamps. Another part of the signal coming out of preamps is passed to postamps where it is further amplified with a gain of 40 db. Hence after passing through postamps the total gain of the signal is 100 db which corresponds to a magnification of 10^5. Here the amplitude of the signal is compared with a preset threshold value. For this work the threshold value was set at 1 volt. A part of the signal (out put of postamp) is then passed to Ringdown Counter/Event duration module (REM) which determines the ring down count and event duration. Another part of this signal is passed to Time Difference Module (TDM) which measures difference in time of arrival of an acoustic emission wavefront at two different sensors. The outputs of TDM, REM and ARM are fed to the computer of AE equipment. Some external analog parameter can also be fed to the computer through Parametric Input/RMS module (PRM). The block diagram of acoustic emission data recording system is shown in Fig. 3.3.
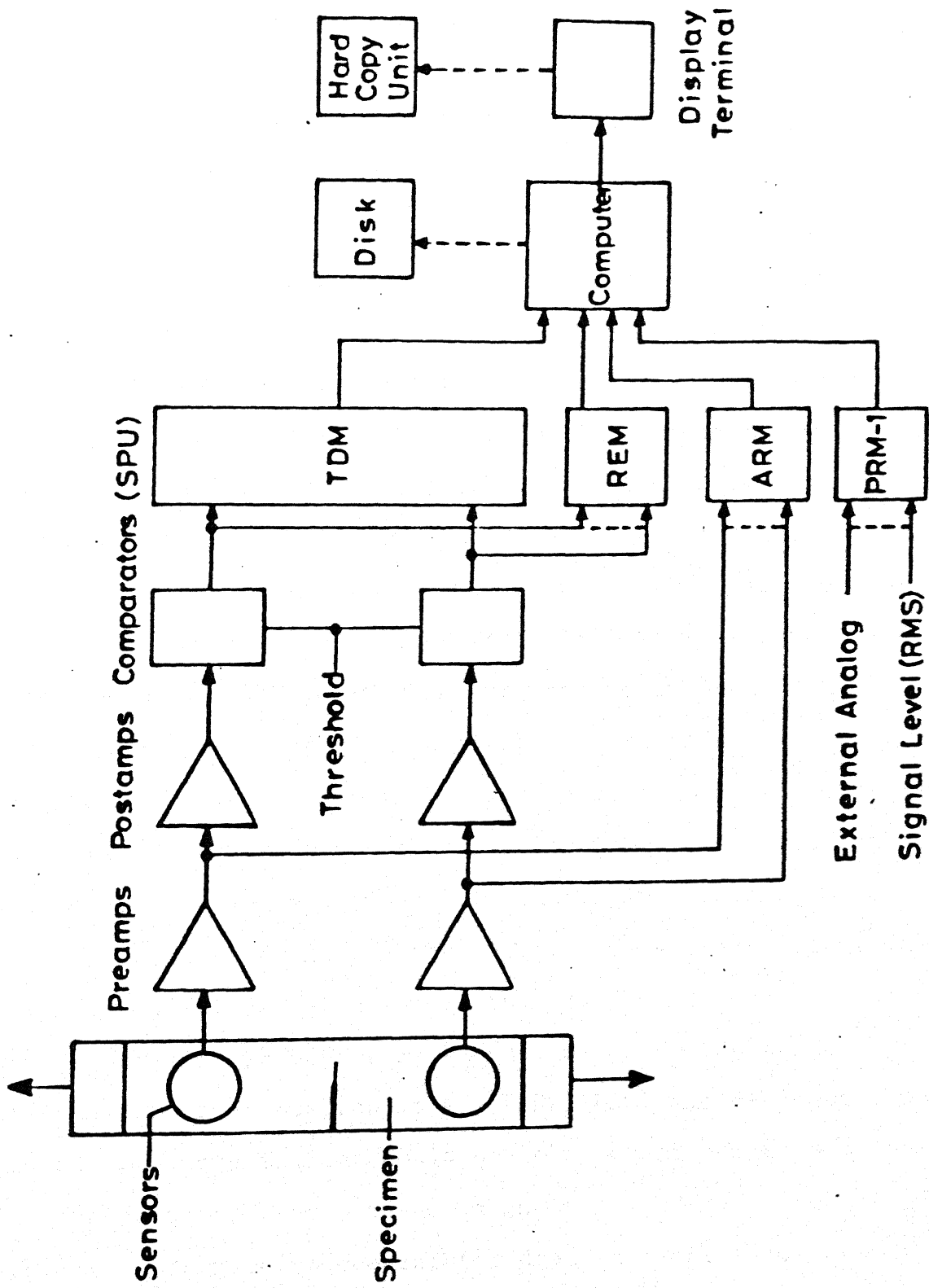
Fig. 3.3. Block diagram of a general acoustic emission system.

A typical record of AE data in the computer is shown in Fig 3.4. The data related to a single event is printed in two lines because of the printer limitations. The sign # indicates that the event is a valid event. TST is for the test no. which is 1 for this case. Sensor indicates the sequence in which the sensors have received the event. For first event it is 12 which indicates that the sensor 1 received the event before the sensor 2. DT1, DT2, DT3, DT4, DT5, DT6 and DT7 are arrival time differences for 8 sensors. However, for the present work only two sensors were used and hence value of DT1 only will be recorded which is 1 micro second for first event. ED is event duration which is 39 microseconds for the first event, PA is peak amplitude which is 44 db for the first event, ENG is energy which is 46 for the first event, RT is rise time which is 8 micro seconds for the first event, SLOPE is 20 db/μs for the first event, Time of the first event is 00:00:00.62 that is 0.62 seconds after starting the test. RG is the region no. which will be same for every event in a linear test with two sensors. For the present work only the events in the region between the sensors have been recorded. LOC is the location of the source of acoustic emission in terms of no. of divisions between two sensors. The region between two sensors for the present work was divided into 100 parts. For the first event, the location is 47. PAR1, PAR2 and PAR3 are external analog parameters which could be load, displacement and strain. In the present case these signals could not be recorded properly. Before proceeding for data analysis this output was rearranged after eliminating columns for DT1 to DT7 as shown in Fig 3.5. The time was stored as T1, T2 and T3 where T1 is hr. T2

ENG	TST RT	SENSOR SLOPE	DT1 EVENT	DT2 TIME	RG	DT3 LOC	DT4 PAR1	DT5 PAR2	DT6 PAR3	DT7	RDC	ED	PA
	# 1	12	1	---		---	---	---	---	---	9	39	44
46	8	20		00:00:00.62	1	47	90	60	200				
	# 1	12	9	---		---	---	---	---	---	3	8	39
34	8	11		00:00:00.64	1	22	90	60	200				
	# 1	12	7	---		---	---	---	---	---	6	33	41
42	18	6		00:00:00.80	1	28	90	60	200				
	# 1	12	1	---		---	---	---	---	---	58	323	76
87	17	370		00:00:00.84	1	47	9?	6?	200				
	# 1	21	8	---		---	---	---	---	---	2	16	32
30	15	3		00:00 ... 8?	1	75	9.	?	200				
	# 1	12	1	---		---	---		---	---	13	51	44
47	8	20		00:00 ... .90	1	'7	9?		200				
	# 1	12	C	---		---	---		---	---	56	241	77
87	5	1413		00:00 ... .91	1	50	90	60	200				
	# 1	21	2	---		---	---	---	---	---	22	67	51
55	7	51		00:00:00.91	1	57	90	60	200				
	# 1	12	5	---		---	---	---	---	---	4	21	39
38	18	5		00:00:00.94	1	34	90	60	200				
	# 1	12	1	---		---	---	---	---	---	22	92	53
59	17	26		00:00:00.96	1	47	90	60	200				
	# 1	12	5	---		---	---	---	---	---	3	18	38
37	1	79		00:00:00.98	1	34	90	60	200				
	# 1	21	1	---		---	---	---	---	---	20	53	52
55	11	36		00:00:00.99	1	54	90	60	200				
	# 1	21	8	---		---	---	---	---	---	9	29	40
41	8	13		00:00:01.07	1	75	90	60	200				
	# 1	21	4	---		---	---	---	---	---	11	41	41
43	10	11		00:00:01.08	1	63	90	60	200				
	# 1	21	3	---		---	---	---	---	---	4	21	35
34	17	3		00:00:01.12	1	60	90	60	200				
	# 1	12	1	---		---	---	---	---	---	47	195	69
78	17	165		00:00:01.13	1	47	90	60	200				
	# 1	21	3	---		---	---	---	---	---	22	65	51
55	8	44		00:00:01.17	1	60	90	60	200				
	# 1	21	8	---		---	---	---	---	---	13	50	43
46	11	13		00:00:01.29	1	75	150	80	200				
	# 1	12	2	---		---	---	---	---	---	7	17	44
42	8	20		00:00:01.37	1	44	150	80	200				
	# 1	12	12	---		---	---	---	---	---	1	1	35
21	1	56		00:00:01.45	1	13	150	80	200				
	# 1	12	3	---		---	---	---	---	---	2	17	36
34	16	4		00:00:01.48	1	41	150	80	200				
	# 1	12	1	---		---	---	---	---	---	7	24	42
42	21	6		00:00:01.51	1	47	150	80	200				
	# 1	12	2	---		---	---	---	---	---	10	25	44
44	8	20		00:00:01.57	1	44	150	80	200				

Fig. 3.4 A typical acoustic emission data set recorded in the computer

SAMPLE:90(12)

PA	ED	RDC	RT	ENG	SLP	PAR1	PAR2	PAR3	TST	SN	DT1	T1	T2	T3	RG	LOC
41	15	6	2	39	56	210	Ø	10	1	12	2	Ø	Ø	Ø.38	1	46
38	4	2	1	30	79	210	Ø	10	1	12	7	Ø	Ø	Ø.39	1	35
57	55	14	6	60	118	210	Ø	10	1	12	1	Ø	Ø	Ø.39	1	48
24	26	2	25	24	1	210	Ø	10	1	21	10	Ø	Ø	Ø.40	1	72
44	21	9	2	43	79	210	Ø	10	1	12	1	Ø	Ø	Ø.41	1	48
53	68	22	24	57	19	210	Ø	10	1	12	4	Ø	Ø	Ø.42	1	41
31	1	1	1	17	35	210	Ø	10	1	12	20	Ø	Ø	Ø.43	1	7
31	1	1	9	17	4	210	Ø	10	1	12	Ø	Ø	Ø	Ø.45	1	50
35	10	2	9	31	6	210	Ø	10	1	12	4	Ø	Ø	Ø.47	1	41
43	42	13	13	45	11	210	Ø	10	1	12	7	Ø	Ø	Ø.47	1	35
37	41	5	1	39	71	210	Ø	10	1	12	4	Ø	Ø	Ø.53	1	41
34	7	3	3	28	17	210	Ø	10	1	12	12	Ø	Ø	Ø.55	1	24
27	65	10	39	31	1	210	Ø	10	1	21	22	Ø	Ø	Ø.55	1	98
60	80	25	9	65	111	210	Ø	10	1	12	6	Ø	Ø	Ø.55	1	37
34	85	21	31	39	2	210	Ø	10	1	21	4	Ø	Ø	Ø.56	1	59
50	68	21	2	54	158	210	Ø	10	1	12	2	Ø	Ø	Ø.56	1	46
53	24	6	5	53	89	210	Ø	10	1	21	5	Ø	Ø	Ø.58	1	61
29	104	16	31	35	1	210	Ø	10	1	21	13	Ø	Ø	Ø.62	1	79
38	125	17	20	45	4	210	Ø	Ø	1	21	7	Ø	Ø	Ø.63	1	66

Fig. 3.5 A typical acoustic emission data set used for analysis

is min. and T3 is sec.

3.4 CLUSTER ANALYSIS :

Objective of data analysis is to identify the internal damage mechanisms on the basis of the recorded acoustic emission event parameters. For this purpose, it is necessary to classify the events it different groups such that the events in a group correspond to certain type of damage mechanism. Cluster Analysis is one of the ways of classifying the events into groups. The groups of events are called clusters.

Clustering could be defined as the process of finding homogeneous subsets in a set of data without any prior information regarding the class membership of individual samples or events. Another definition of clustering is the process of grouping various elements in a data set into subsets such that each point in a subset is more similar, in some sense, to other points in that subset than the points in other subsets in the data set.

For a given data set D of N events $(x_1, x_2, \ldots x_n)$, to be classified into K clusters, the process of clustering can be mathematically stated as to seek the clusters C_1, C_2, $\ldots C_k$, such that every x_i, $i = 1, 2 \ldots N$, fall into one of these clusters and no x_i falls in two clusters.

3.4.1 CLUSTERING METHOD :

Clustering methods could either be hierarchical or non-hierarchical. In hierarchical clustering, the sequence of forming clusters proceeds in such a way that whenever two samples

are put into a cluster at some stage, they remain together at all subsequent stages. In the non-hierarchical method, some initial seed points are chosen/obtained and the cluster memberships are altered with respect to certain criteria, before the final clusters are obtained.

For the present work, a non-hierarchical clustering procedure has been used. It is a two step process. All the events are first divided into the desired number of clusters and the events are then shuffled into different clusters to minimize within-cluster sum of squares of deviations from their respective means. Euclidean distance has been taken as the criterion of deviation between the mean and a point. The euclidean distance between two points A and B in a multi variable space is defined as :

$$d(A,B) = [\sum_{i=1}^{J} (A_i - B_i)^2]^{1/2}$$

where variables A_i and B_i are the magnitudes of ith variables at points A and B. For dividing the events into desired no. of clusters some initial seed points or cluster centers are needed. The overall mean vector of the data set is chosen as the first seed point. The data units are then examined in their input sequence. The data unit, which is at least some specified distance, say d_{th} away from all previously chosen seed points is taken as the next seed point. This process is continued until the required no. of seed points have been chosen or the data set is exhausted. The distance d_{th} is called threshold distance. For a correctly chosen value of d_{th}, desired

number of clusters will be formed from all the data points such that no data points are left out. However, if d_{th} is too small, it will not be possible to assign all the data points to one of the clusters and some data points will be more distant from all the cluster centres than the chosen value of d_{th}. On the other hand, if d_{th} is too large, the number of seed points will be less than the number of clusters desired. In either of these two cases the value of d_{th} is changed from the first assumed value.

Initially the threshold distance is chosen to be :

$$d_{th} = 1/N \ [\ \sum_{i=1}^{J} \ (R_i)^2 \ ]^{1/2}$$

where,

N : Number of clusters

J : Number of variables

R : Range of variables

The second step in forming clusters involves minimising deviations within clusters. For this purpose, individual events are shuffled between different clusters and each time within-clusters sum of squares of deviations from their respective means is examined. If shifting of an event results in the reduction of the deviation, the event is retained in the new position otherwise it is shifted back to its old cluster. When the event is assigned to a new cluster, the new cluster means are calculated. This process is repeated until all the events are examined and assigned to the most apropriate cluster so that deviations are minimum.

3.4.2 Choice of Variables :

The choice of variables influencing formation of clusters is extremely important. Since clusters are expected to be related to different types of damage mechanisms, all the parameters related to the type of damage must be included as variables in analysis. On the other hand, to minimise the analysis time the total number of variables should be as small as possible. This is accomplished by eliminating the parameters that are unrelated to the damage mechanism and the parameters that are related to other parameters.

Out of the recorded parameters, time and location of damage are not related to the type of damage and hence excluded from the cluster analysis. Further, it appears that ENG is related to PA and RDC to RT since their variations are similar. Therefore, PA and RT have been picked up for further analysis leaving out ENG and RDC. The slope (SLP) has also been excluded from analysis since it is calculated from PA and RT. Thus, only three parameters namely, PA, RT and ED have been considered as indepent variables related to the damage mechanisms and, therefore, used for cluster analysis.

3.4.3 Normalizing the variables :

Ranges of numerical values of different variables are different because of their units. The variables with larger ranges of numerical values will have a more dominant influence on the formation of clusters and thus introduce a bias in the data analysis. In the present case this bias has been eliminated by

normalising the numerical values of variables with respect to the range of values of the variable for an event.

3.4.4 Software description :

Computer codes used in the cluster analysis were developed by Ravi Kumar (28). They are briefly described below :

FORMAT.FOR : To rearrange the recorded data after removing parameters DT2 to DT7.

SEED.FOR : To obtain the ranges of variables and guess the initial threshold distance.

BALL.FOR : To obtain the initial seed points. The program needs three primary inputs : number of events, number of variables, number of seed points required and threshold distance.

SCL.FOR : This is the main program, which for a given matrix of I events on J variables, allocates the events to N clusters in such a way that the within-cluster sum of squares of deviations from their respective means is minimized. The primary inputs are : matrix of recorded events [I,J], the number of clusters N, and the initial cluster centres [N,J].

CHAPTER 4

RESULTS, ANALYSIS AND DISCUSSION

Fatigue behaviour of carbon fabric reinforced epoxy composite has been studied. The composite plates made in laboratory had about 46% fibers by volume. Static and fatigue tests were conducted in a 10 ton servohydraulic material testing system (MTS model 810). Fatigue modulus was continuously recorded to study damage propagation. Internal damage mechanisms such as matrix cracking, fiber breaking and delamination were studied using acoustic emission technique. For this purpose some controlled experiments were also carried out.

4.1 STATIC BEHAVIOUR:

Static tension tests on specimens of carbon/epoxy composite were conducted in MTS testing system under load control with loading rate of 5 KN/min. An extensometer of gauge length 25 mm was used to measure the strain. Tests were controlled through a PC which also recorded the load and strain values. A typical stress-strain curve is linear upto failure (Fig. 4.1). The modulus based on initial slope of stress-strain curve and strength based on peak load are automatically calculated through software available in the PC.

Results of the tension tests (Table 4.1) showed that the strength exhibit considerable variation from plate to plate. Therefore, the tests were conducted on at least3 specimens taken from each of the plate cast. A total of 37 specimens were tested. Their average ultimate tensile strength was found to be 1089 MPa. For some specimens modulus was also found. The average static
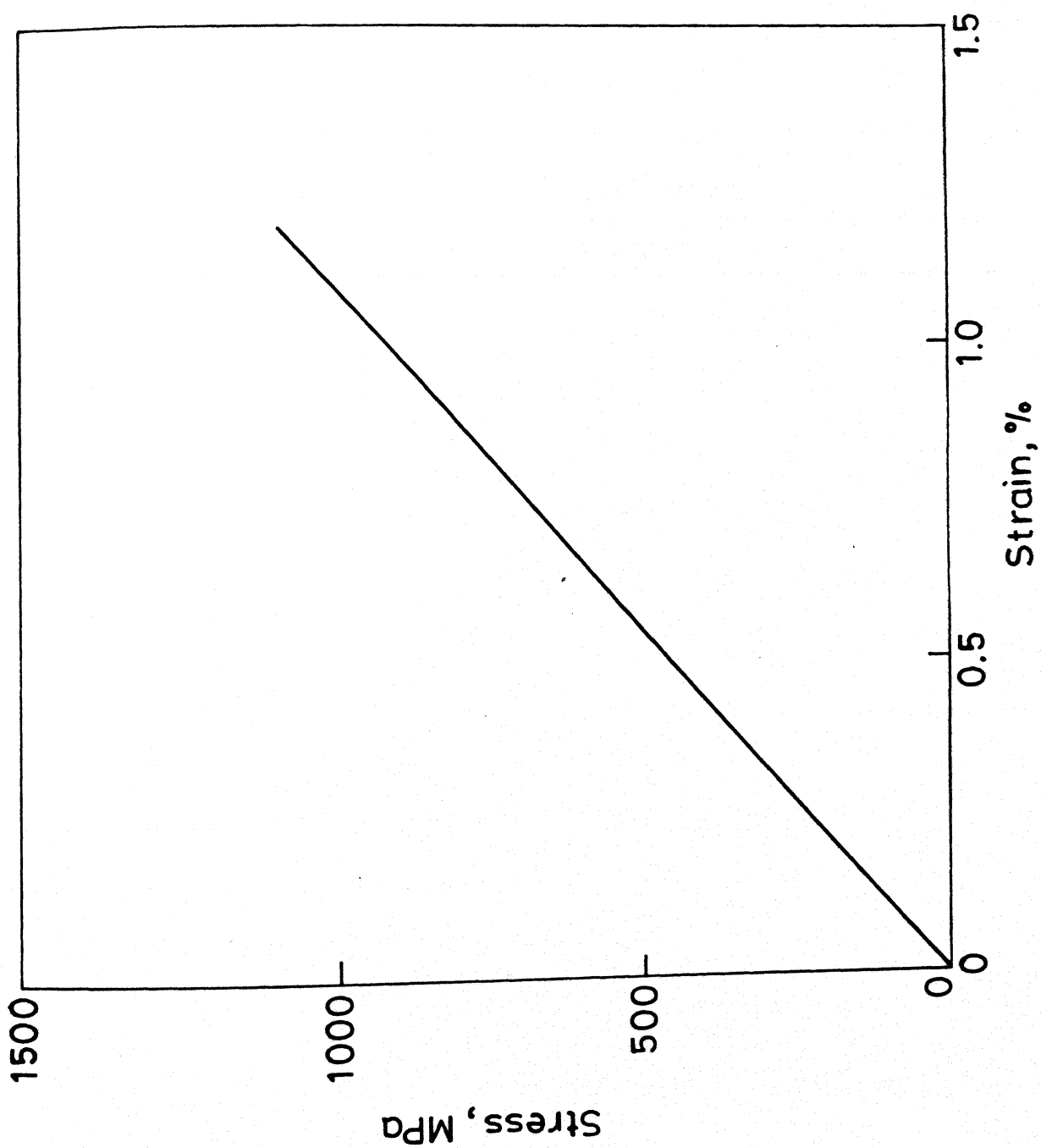
Fig. 4.1 A tyical stress vs strain curve during static tensile test.

Table 4.1

| Static Tensile Strengths of the specimens (MPa):									
926,	929,	958,	965,	1042,	946,	1117,	1049,	1087,	1179,
1192,	978,	1078,	1050,	1035,	1034,	1111,	1031,	1007,	1016,
1145,	1245,	1306,	1162,	1061,	1241,	1247,	1231,	1212,	1041,
1042,	1212,	1130,	1073,	1139,	1016,	1031			
Average static tensile strength = 1079 MPa									

modulus was 96 GPa. For the purpose of calculating maximum stress to be applied during fatigue tests on specimens from a particular plate, the average tensile strength of that plate was considered.

In static tests different specimens failed in different ways. Typical failure modes are illustrated through photographs of the failed specimens (Fig.4.2). In some specimens failure occurred with fibers fracturing in one cross-section only while in other specimens, fibers fractured at more cross-sections and a matrix crack parallel to the fibers joined them. Some of the specimens broke into pieces more than two also.

4.2 FATIGUE LIFE :

The fatigue tests were conducted between fixed stress limits of tension-tension sinusoidal loading and a stress ratio R = 0.1. Initial tests were conducted to select appropriate frequency for fatigue tests so that failure would occur in the test section, that is, away from the end tabs. Further, for studying damage through acoustic emission technique, stress levels were chosen so that the fatigue life was around 1000 cycles. For very long life, the number of acoustic emission events will be very large due to both the new damage events and fretting between already created surfaces. This causes difficulty in recording events and in classifying them. If fatigue life is very small, acoustic emissions from different damage mechanisms overlap and get recorded as a single event. Thus, the damage identification and data analysis becomes difficult. Most of the specimens tested at a frequency of 10 Hz (Smax = 0.9 Su and 0.85 Su) failed outside the test section (either very close to or inside the end
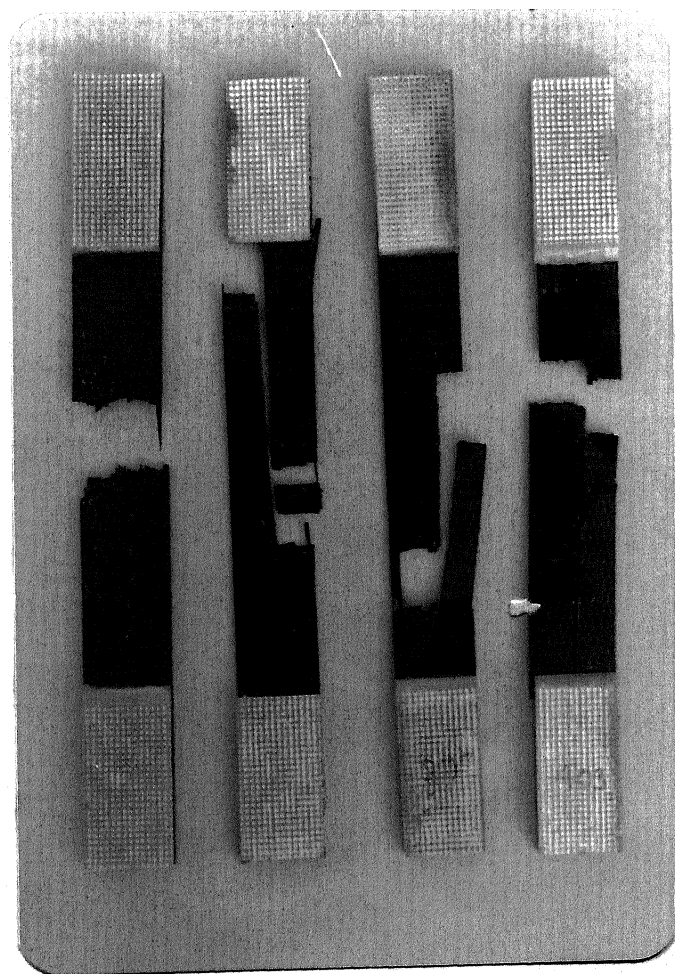
(a)   (b)   (c)   (d)

Fig. 4.2. Specimen failed during tensile tests

tabs). Some of the specimens tested at a frequency of 1.5 Hz and Smax = 0.9 Su showed a fatigue life of around 50,000 cycles which is too long for damage monitoring. Most of the specimens tested at a frequency of 1.5 Hz and Smax = 0.9 Su failed inside the test section and showed fatigue life in the desired range. Fatigue lives of specimens are given in Table 4.2. There is a lot of scatter in fatigue life data. Scatter in fatigue life data of composite materials has been observed by many investigators including Agarwal and Majumdar (27). It is to be noted here that the specimens tested at 10 Hz frequency generally showed failure outside the test section and therefore no conclusion should be drawn from these results. 25 specimens were tested at Smax = 0.9 Su and f = 1.5 Hz. Failure modes are illustrated through photographs of some of the failed specimens tested at Smax. = 0.9 Su and f = 1.5 Hz in Fig. 4.3. Generally all the specimens failed at one cross section. Some of the specimens showed delamination before failure.

4.3 DAMAGE BASED ON FATIGUE MODULUS DURING FATIGUE LOADING :

In the present fatigue tests, specimens were subjected to load cycles with fixed stress limits while the strain limits varied. Stress-strain curve for the cyclic loading is represented schematically in Fig.4.4. The ratio of applied stress to resultant strain defines the fatigue modulus (29,30) at a specified cycle. That is, the slope of line AN shown in Fig. 4.4 is the fatigue modulus, F(N), at cycle N. Due to microscopic damage, fatigue modulus of the composite decreases continuously. It can be easily calculated without interrupting the fatigue

Table 4.2

Sl no.	Cyclic Life N_f	Whether Failure Occured in Test Section
S_{max} = Ø.85 Su, f = 1Ø Hz.		
1	14ØØ	No
2	12ØØ	No
3	1116	No
4	4Ø74	No
5	1323	No
Average life = 1822.6 cycles		
S_{max} = Ø.85 Su, f = 1.5 Hz.		
1	1735	No
2	273	Yes
3	3968	No
4	37816	Yes
5	14116	No
6	57Ø7Ø	Yes
7	51Ø11	Did not fail
8	1366Ø	Yes
9	571	Yes along len.
Average life = 2ØØ24 Cycles		
S_{max} = Ø.9 Su, f = 1Ø Hz.		
1	14Ø4	No
2	1Ø83	No
3	1498	No
4	621	No
5	7Ø5	No

Average life 1062.2 Cycles		
S_{max} = 0.9 Su, f = 1.5 Hz.		
1	1035	Yes
2	580	Yes
3	1343	No
4	6923	No
5	31333	No
6	7131	Yes
7	428	Yes along len.
8	2582	Yes
9	62	Yes
10	2398	Did not fail
11	44	No
12	4906	Yes
13	1959	No
14	6744	Did not fail
15	5620	Did not fail
16	15853	Yes along len.
17	369	Yes
18	636	Yes
19	400	Did not fail
20	7428	Yes
21	574	Yes
22	1771	Yes
23	2239	Yes
24	5010	Yes
25	1030	Yes
Average life = 4335.92 Cycles		
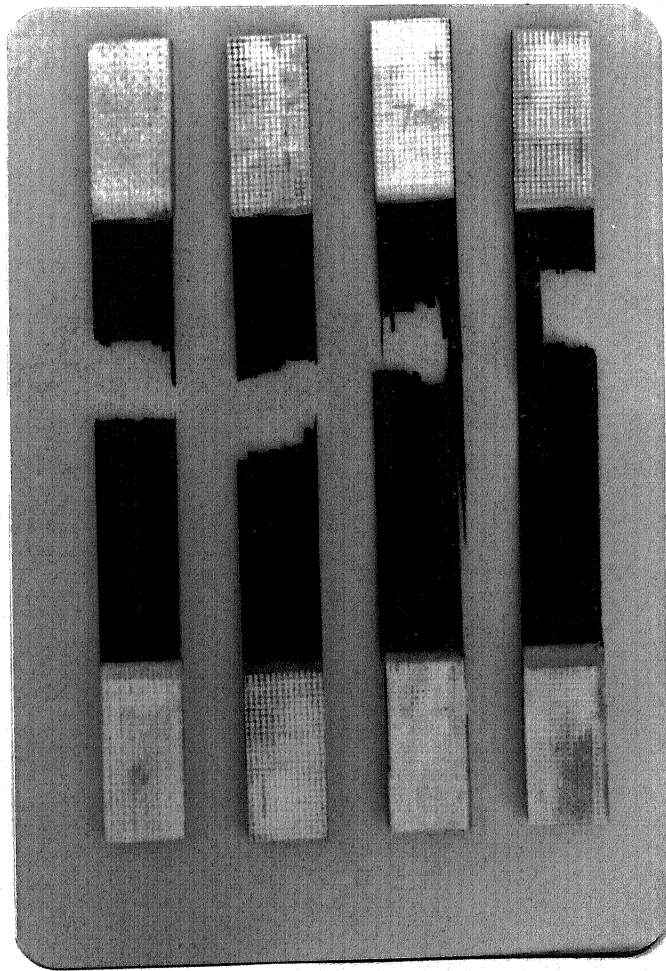
(a)   (b)   (c)   (d)

Fig. 4.3 Specimen failed during fatigue tests

Fig.4.4 Schematic representation of fatigue modulus.

test. Consequently, the fatigue modulus is considered a good parameter to represent the extent or severity of fatigue damage.

For the purpose of studying damage throughout the life of a specimen, normalized damage, D, and normalized number of cycles, N^* have been defined below such that they vary between 0 and 1 :

$$D = \frac{F(1) - F(N)}{F(1) - F(N_f)}$$
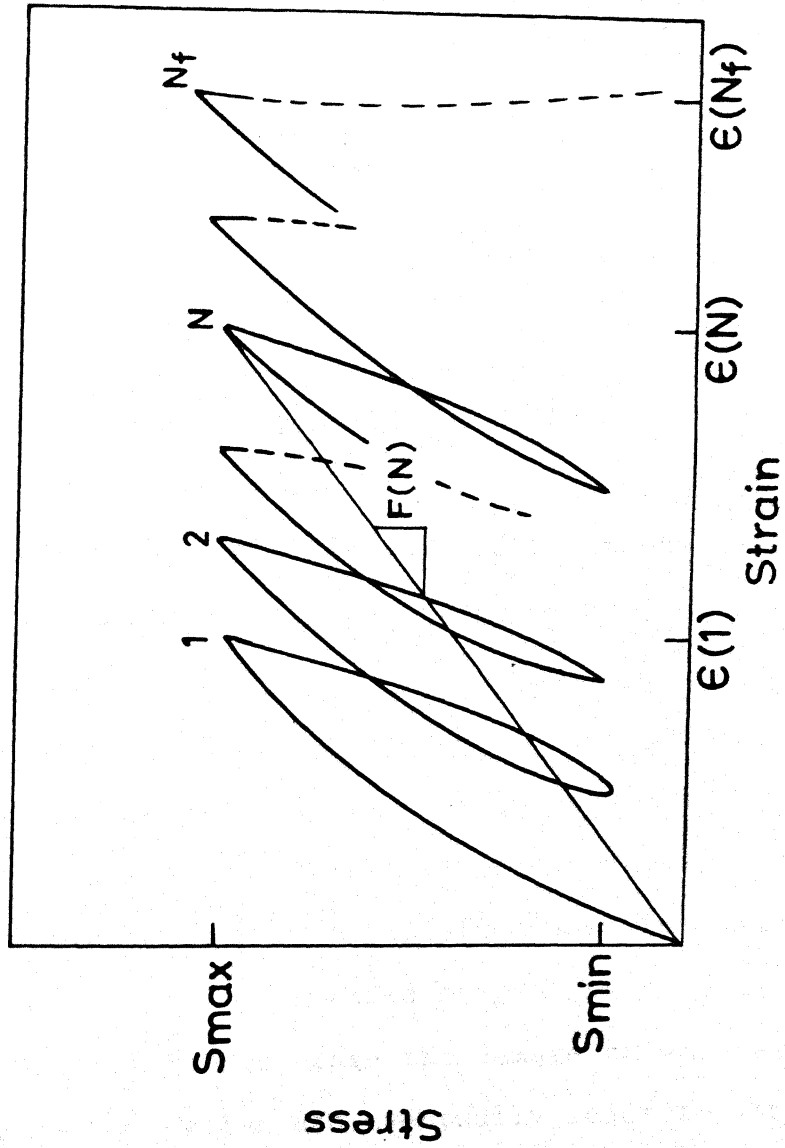
and

$$N^* = \frac{N - 1}{N_f - 1}$$

Where N_f is the fatigue life. A typical plot of normalized damage, D, against the normalized number of cycles, N^*, for a specimen tested at $S_{max} = 0.9Su$ and 1.5 Hz frequency is shown in Fig.4.5. It is observed that the damage is progressive. In stage I damage initiates rapidly and then accumulates at progressively lower growth rates. This stage may be referred to as the damage initiation stage. In stage II the damage growth rate is very low and thus, it is the steady damage stage. In stage III, the damage starts increasing again probably after a threshold damage is reached in stage II. This third stage is called the damage propagation stage. In this stage the damage growth rate increases with the number of cycles and eventually leads to the specimen failure. Similar behaviour has been observed by Agarwal and Majumdar (27) for Kevlar/epoxy composite. The beginning of damage propagation stage may be compared with the appearance of a crack in metals during fatigue loading. A detectable crack in metals grows rapidly and causes fatigue failure. In composites, the
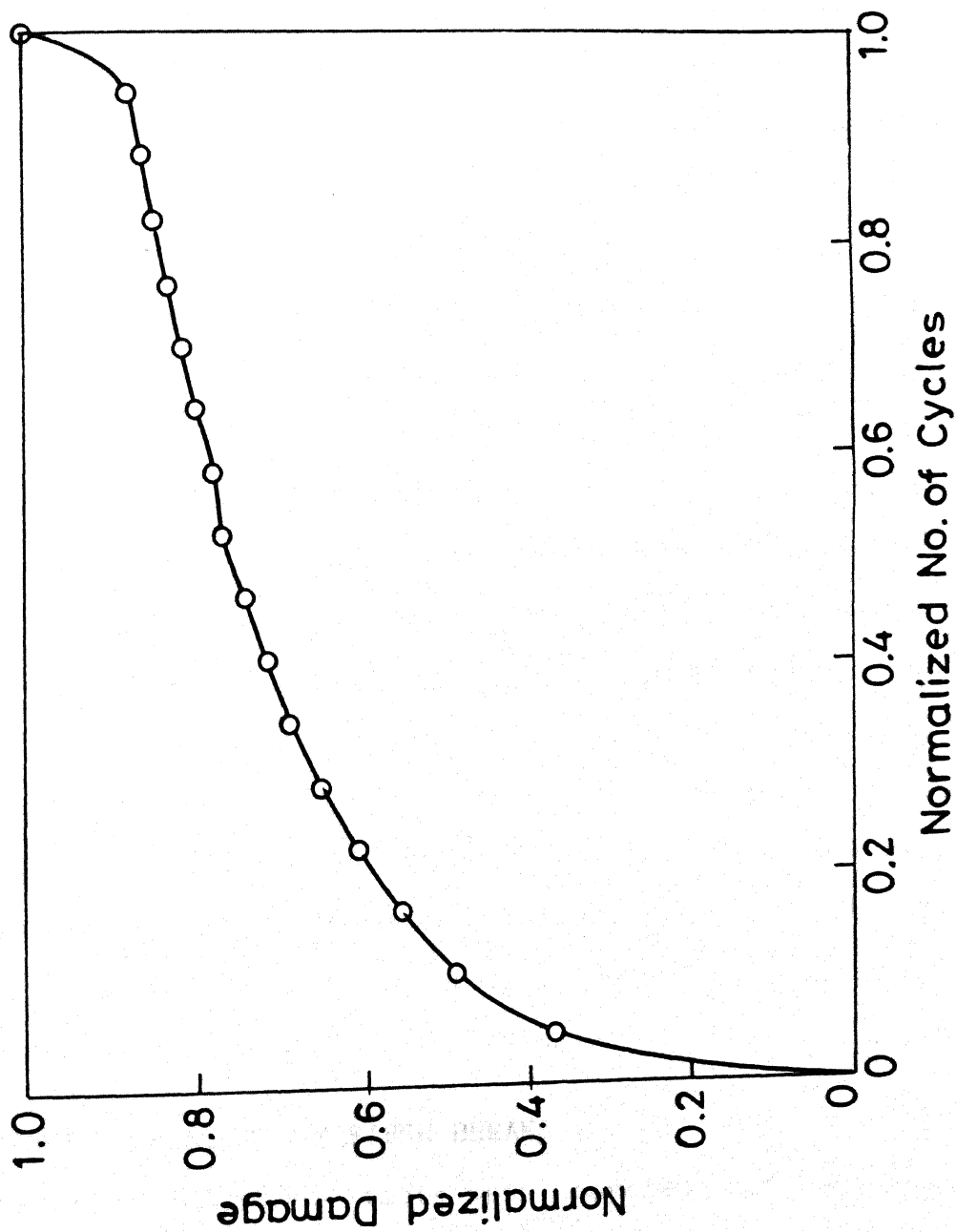
Fig. 4.5 A typical damage curve.

beginning of damage propagation stage may similarly signify an unsafe structure. The present studies have been focussed to identify the begining of the third stage of damage.

4.4 IDENTIFICATION OF ACOUSTIC EMISSION CHARACTERISTICS OF INTERNAL DAMAGE MECHANISMS :

When composite materials are subjected to fatigue loading, internal damage occurs due to fiber breaking, matrix cracking, delamination and debonding. These may occur separately or in combination, e.g. fiber pull-out is a combination of fiber break and debonding. To identify these damages through acoustic emission records during a test, there is a need to identify the acoustic emission characteristics of the internal damage mechanisms. It is accomplished by conducting tests in which damage of one type is predominant. The aim of such experiments is to identify characteristic acoustic emission parameters for each type of damage so that during normal fatigue test the type of damage can be identified for every recorded event on the basis of these parameters. Such controlled experiments have been performed on specimens in which predominant failure modes are fiber breaks, matrix cracks and delamination respectively. The results of these experiments are presented in following sections.

4.4.1 CHARACTERISTICS OF FIBER BREAKS :

For this purpose, tests were carried out on specimens prepared such that the specimens in their mid-length region had fibers only and no resin so that fiber breaks will be predominant damage mechanisms. The average static strength of such specimens was found to be 505 MPa which is much lower than that of the
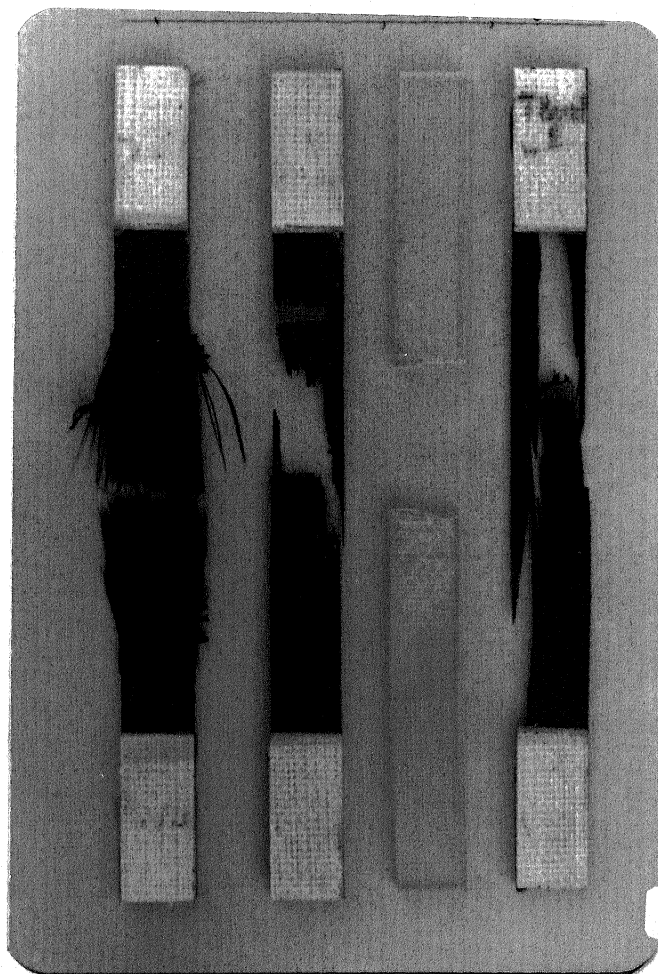
(a)　　　(b)　　　(c)　　　(d)

Fig. 4.6.　Specimens failed during controlled experiments

(a) Specimen for fiber break
(b) Specimen for delamination
(c) Specimen for matrix cracks
(d) Unidirectional specimen

Table 4.3   Cluster Analysis of Fibre Break Specimens

CLUSTER NO.	NO. OF EVENTS	MEAN AE PARAMETERS		
Specimen 1				
		PA	ED	RT
1	733	49.1	18.3	4.9
2	323	58.3	70.4	16.6
3	63	61.6	182.4	37.8
4	15	9.3	520.0	95.0
5	6	59.7	376.5	78.8
Specimen 2				
1	713	48.0	17.8	4.4
2	547	56.6	60.7	14.9
3	74	62.1	171.2	34.7
4	16	28.9	509.8	90.2
5	226	60.6	105.9	23.4
6	42	63.3	281.2	53.8

Table 4.3   Cluster Analysis of Fibre Break Specimens

CLUSTER NO.	NO. OF EVENTS	MEAN AE PARAMETERS		
		PA	ED	RT
Specimen 1				
1	733	49.1	18.3	4.9
2	323	58.3	70.4	16.6
3	63	61.6	182.4	37.8
4	15	9.3	520.0	95.0
5	6	59.7	376.5	78.8
Specimen 2				
1	713	48.0	17.8	4.4
2	547	56.6	60.7	14.9
3	74	62.1	171.2	34.7
4	16	28.9	509.8	90.2
5	226	60.6	105.9	23.4
6	42	63.3	281.2	53.8

normal specimens. Fatigue loading with stress ratio R = 0.1, frequency f = 1.5 Hz was applied. Since there was lot of scatter in the static strength values, the fatigue tests were started with a low value of maximum stress (S_{max} = 0.5 Su) which was gradually increased to a level that produced detectable acoustic emissions. Photograph of one such specimen after failure is shown in Fig. 4.6a. Acoustic emission data were collected during fatigue loading of two such specimens. The cluster analysis results for the data are presented in Table 4.3. For both the specimens, there is one cluster each with large no. of events (64.3% of total events for one specimen and 44.1% for the other). These clusters correspond to a low value of event duration (ED = 18.3 for specimen no. 1 and ED = 17.8 for specimen no. 2). Since fiber breaks are expected to be the predominant mode of internal damage mechanism, it was assumed that the events corresponding to a low value of ED (between 0 to 25) represent fiber breaks. This may be expected from theoretical considerations also. That is, the fibers have a small cross sectional area and their fracture is brittle so that a fiber break is expected to produce an acoustic emission of small duration and hence a low ED.

4.4.2 CHARACTERISTICS OF MATRIX CRACKS :

For this purpose tests were conducted on unreinforced epoxy specimens. Average ultimate tensile strength of the material was found to be 40 MPa. For these specimens fatigue loading with R = 0.1 and f = 1.5 Hz was applied. While starting the test, the maximum stress level was kept at 0.5 Su which was increased till the specimen started emitting detectable acoustic signals. At

first, some specimens with a triangular notch were tested. These specimens produced only 5 to 10 acoustic emission events during entire cyclic life. However, to get complete range of acoustic emission parameters for matrix cracks, a larger number of events is required. Therefore, unnotched specimens with surface scratches in the middle region were tested. Scratches are visible in the photograph of the specimen taken after failure (Fig. 4.6b). Cluster analysis results of the data are shown in table 4.4. The values of ED of the means of the three clusters are 101.6, 48.5 and 160.1. It should be noted that there is no cluster with low ED which would represent fiber breaks. Since specimen is made of unreinforced epoxy, the recorded acoustic emission events should only be from matrix cracks. Therefore, the events corresponding to this wide range of ED (between 25 to 200) are assumed to represent matrix cracks. This may be expected from theoretical considerations also. That is, in a specimen, matrix cracks perpendicular to the direction of loading can propagate much faster than those along the direction of loading. Therefore, significant variation in the event durations is possible for matrix cracks.

4.4.3 CHARACTERISTICS OF DELAMINATION :

For this purpose a test was carried out on a specimen in which milar sheet pieces were inserted between laminae at the time of its fabrication. The milar sheet does not get bonded to the epoxy resin and thus promotes delamination during loading. Fatigue loading with R = 0.1 and f = 1.5 Hz was applied. While starting the test the maximum stress level was kept at 0.5 Su

Table 4.4 Cluster Analysis for Matrix Crack Sp. 1.

CLUSTER NO.	NO. OF EVENTS	MEAN OF THE CLUSTER		
		PA	ED	RT
1	238	43.9	101.6	18.7
2	313	35.1	48.5	10.9
3	266	44.3	160.1	27.5

Table 4.5 Cluster Analysis of Delamination Sp. 1.

CLUSTER NO.	NO. OF EVENTS	MEAN OF THE CLUSTER		
		PA	ED	RT
1	167	63.0	119.5	27.3
2	34	65.3	227.1	46.8
3	149	51.3	48.0	10.5

which was increased gradually. The delamination was clearly visible throughout the specimen between different layers. Photograph of the specimen taken after failure is shown in Fig. 4.6b. Photograph of side of the middle portion of the specimen taken after failure is shown in Fig. 4.7a. The specimen is certainly expected to produce acoustic emissions caused by delamination. However, the recorded data would contain acoustic emission events caused by fiber breaks and matrix cracks as well. Delamination cracks are long since they occur in a plane parallel to the fibers and hence, are not arrested by fibers. It may therefore be expected that the event duration for delamination be longer than that for other events. The number of delamination events is expected to be small because they occur only on lamination planes between two laminae whose number is limited whereas other events take place throughout the specimen. The cluster analysis results of the data are shown in table 4.5. There is one cluster with a very high value of ED (ED 227.1). In this cluster, the number of events is 34 out of a total of 350. This clusters with so high ED and small number of events is expected to be of delaminations as discussed above. Other clusters have very large no. of events with ED corresponding to the matrix cracks and fiber breaks.

Characteristics of delamination were obtained from another specimen tested later which showed extensive delamination .This specimen was tested at Smax = 0.9 Su, f = 1.5 Hz and R = 0.1 and showed a fatigue life of 15853 cycles. Photograph of the specimen edge taken after failure is shown in Fig. 4.7b. It was observed
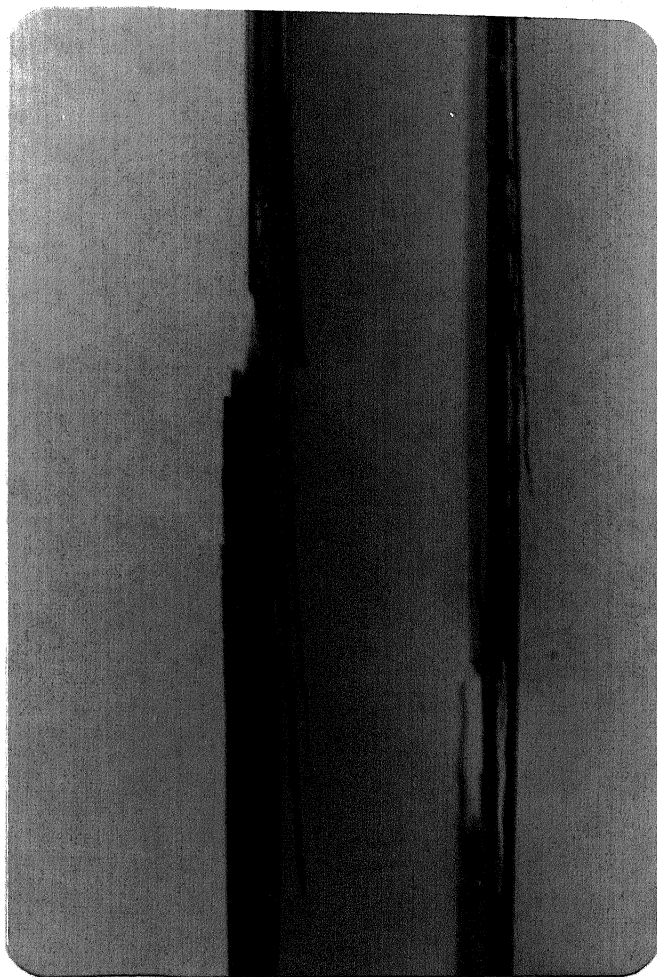
(a)　　　　　(b)

Fig. 4.7.　Side　view of specimens　used　to
study delamination

(a)　Specimen with milar sheet
inserted between layers
(b)　CFRP Specimen

Table 4.6 Cluster analysis of carbon/epoxy specimen

15000 to 15146 cycles				
CLUSTER NO.	NO. OF EVENTS	MEAN AE PARAMETERS		
		PA	ED	RT
1	801	44.9	60.4	14.8
2	759	40.8	32.8	7.6
3	563	50.8	91.9	23.3
4	360	53.3	125.0	29.6
5	58	56.5	237.0	51.0
6	146	53.1	169.2	37.1
7	7	60.0	344.1	68.7
8	1	55.0	520.0	95.0
9	767	36.3	8.3	2.7
15400 to 15584 cycles				
1	1023	46.8	76.3	18.8
2	593	51.6	116.9	27.7
3	189	53.5	181.9	39.8
4	30	58.0	334.1	69.3
5	1147	42.0	42.6	10.2
6	1264	36.8	11.5	3.3
15749 to 15853 cycles				
1	1347	42.6	49.4	11.6
2	921	48.2	87.1	21.3
3	168	52.7	210.1	44.4
4	12	31.8	441.8	82.7
5	476	50.5	133.3	30.1
6	1362	37.3	13.0	3.5

visually that significant delamination took place just before failure. since data were recorded on several floppies, some data were lost during changing of floppies. Acoustic emission data could be recorded during 15000 to 15146 cycles, 15400 to 15584 cycles, and 15740 cycles to 15849 cycles, that is, until failure failure. The cluster analysis results are given in table 4.6. On the basis of the criterion that ED greater than 200 represents delamination, there are 7, 30 and 168 delamination events in the three parts of life mentioned above. This indicates that the number of delamination events is very low at 15000 cycles and increases at an accelarated rate. By theoretical considerations also it is clear that most of the delamination events will take place towards the end of life only. It is due to delamination that the specimen weakens considerably and eventually fails. As mentioned above, the delamination was visually observed just before failure.

It may be pointed out here that basically, delamination is also a matrix crack caused by shear failure and therefore the event duration (ED) for this crack will be comparatively large. However, because of the importance of delamination in load carrying capacity of the material it is desirable to identify delamination as distinct from other matrix cracks. Due to delamination, adjacent layers of a laminate cease to act together as one unit.

4.4.4 DISCUSSION ON RESULTS OF CONTROLLED EXPERIMENTS :

The results described in the preceding section indicate that fiber breaks, matrix cracks and delamination cracks can be

identified from acoustic emission records on the basis of event duration. The events with ED less than 25 are likely to be fiber breaks, events with ED between 25 and 200 matrix cracks and the events with ED more than 200 delamination cracks. Controlled experiments for fiber breaks are expected to show large no. of fiber breaks, some matrix cracks (in the areas where resin was present) and a few delaminations (likely to develop in the regions adjacent to the no-resin area of the specimen). Results presented in tables 4.3 show this pattern of damage events. Tests on unreinforced resin specimens will show only matrix cracks. Consequently, only matrix cracks are predicted from the results of table 4.4.

4.5 STUDY OF DAMAGE GROWTH THROUGH ACOUSTIC EMISSION :

As already indicated in a previous section, for the purpose of studying damage growth through acoustic emission technique, 7 carbon/epoxy composite specimens were subjected to cyclic loading with Smax = 0.9 Su, R = 0.1, and f = 1.5 Hz. Acoustic Emission data during fatigue loading were recorded on floppies since the hard disc of AET - 5000 data recording system was not functioning. Only about 4300 events can be recorded on a single floppy. The specimens with lives longer than 1000 cycles usually produced more than 4000 events and therefore acoustic emission data had to be recorded on several floppies. For such specimens, some of the acoustic emission data were lost during changing of floppies. Analysis of these incomplete data was not carried out. Complete acoustic emission data for two of the specimens which showed fatigue lives of 237 and 849, could be

recorded for their entire life on a single floppy. These data have been analysed further and discussed in the following paragraphs.

Recorded acoustic emission events were first classified on the basis of ED into three categories representing three damage mechanisms. An event with ED less than 25 represents a fibre break, with ED between 25 and 200 a matrix crack, and with ED more than 200 a delamination crack. The damage growth by each of these mechanisms as represented by numbers of AE events caused by them is shown in Figs. 4.8 and 4.9 for the two specimens. It is observed that each type of damage occurs throughout the fatigue loading and accumulates until failure. For both specimens the number of matrix cracks is highest while delamination cracks are very few.

Each type of damage has been normalized with respect to the maximum damage before failure of the specimen and plotted against normalized number of cycles in Figs. 4.10 and 4.11 for the two specimens. For both the specimens the normalized damage due to fibre breaks and matrix cracks appears to grows steadily until failure. The damage due to delamination grow in random discrete steps which is probably due to the fact that the number of delamination events is very small (22 delamination events in a total of 3126 events for one specimen and 15 out of 2775 events for the other specimen). Due to these small number of delamination events and also due to the fact that the cumulative energy associated with the delamination events is small (Fig. 4.12 and 4.13), no conclusion can be drawn regarding importance of these delamination events towards overall damage severity.
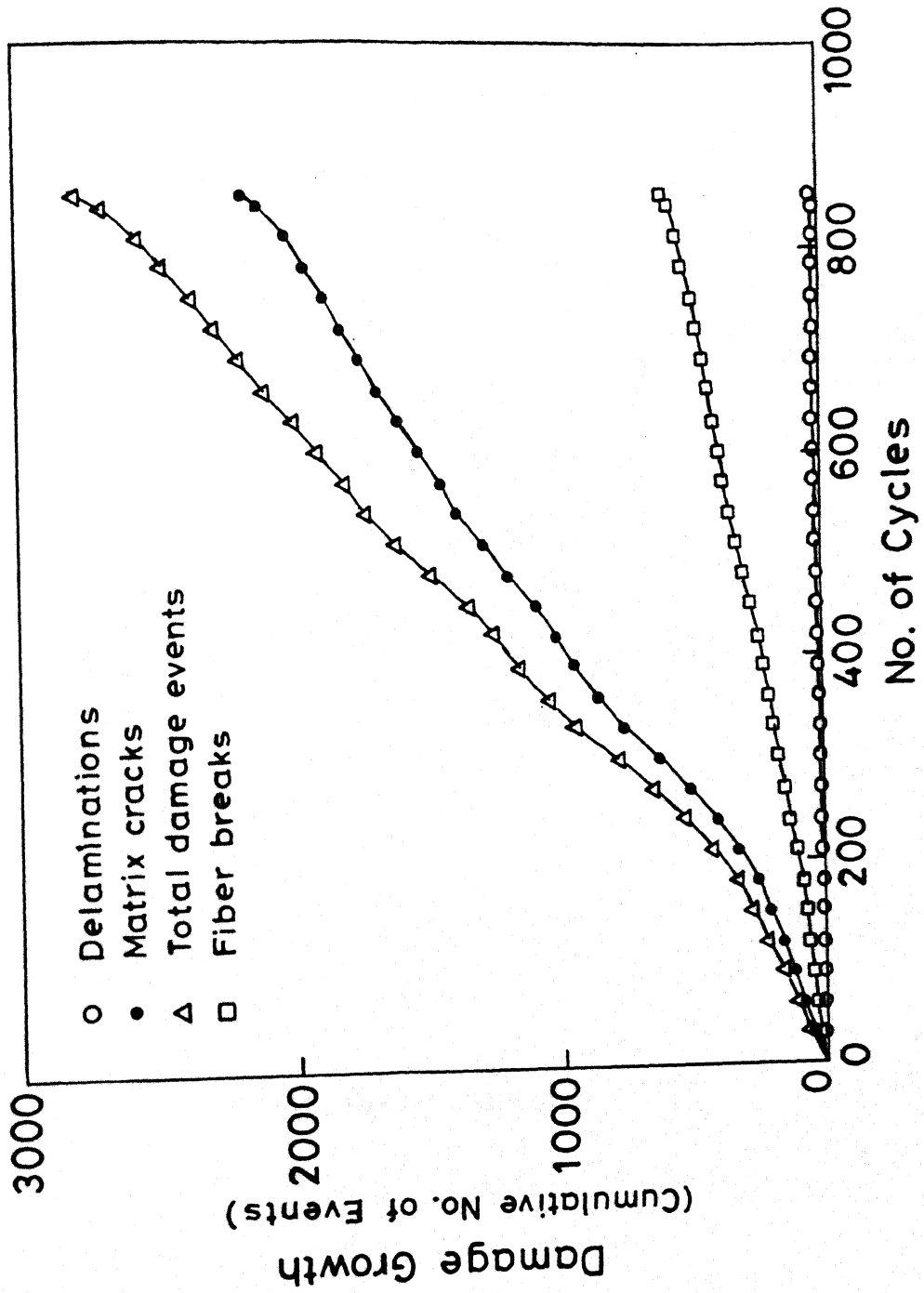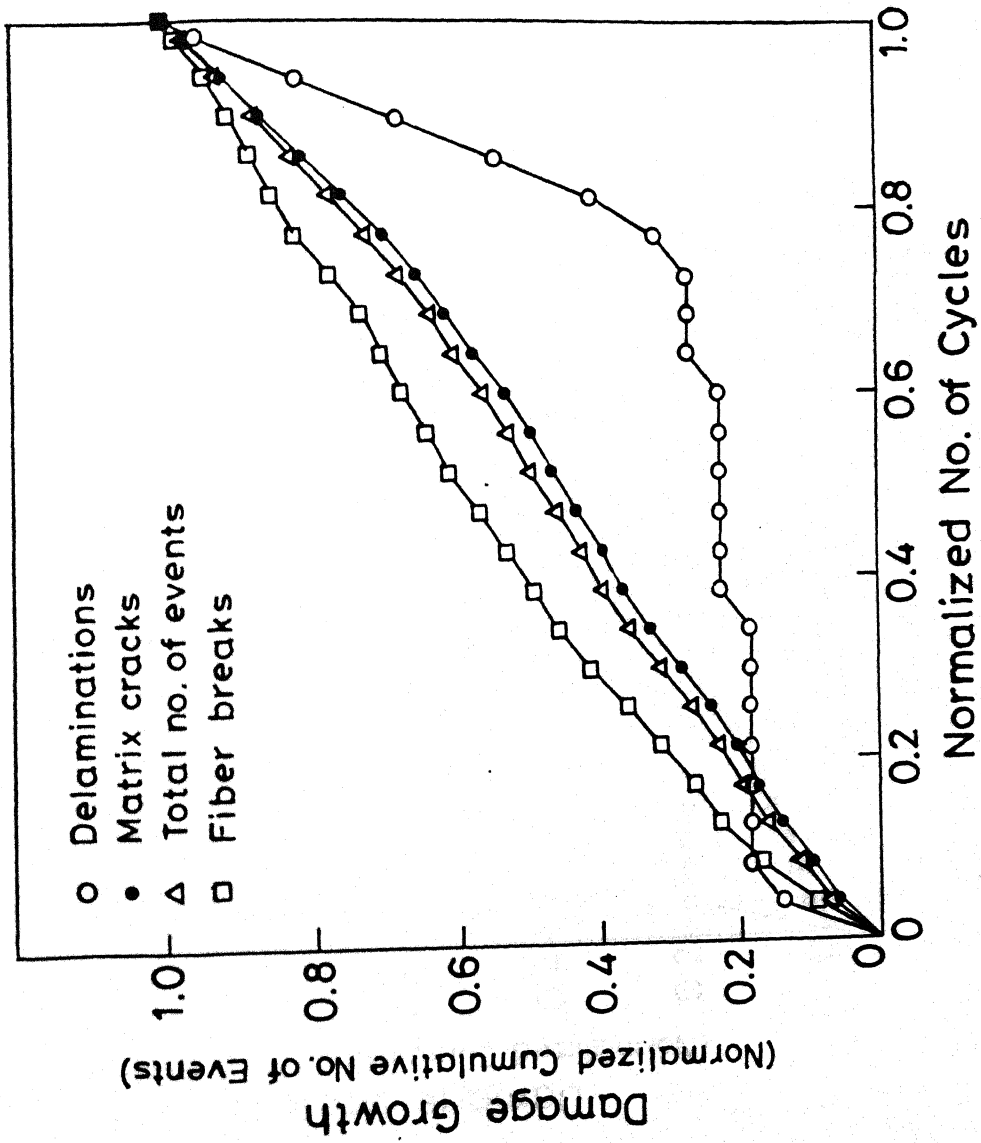
Fig. 4.9 Damage growth in a specimen with $N_f = 849$

Fig 4.10 Normalized damage growth in a specimen with
$N_f = 237$

63
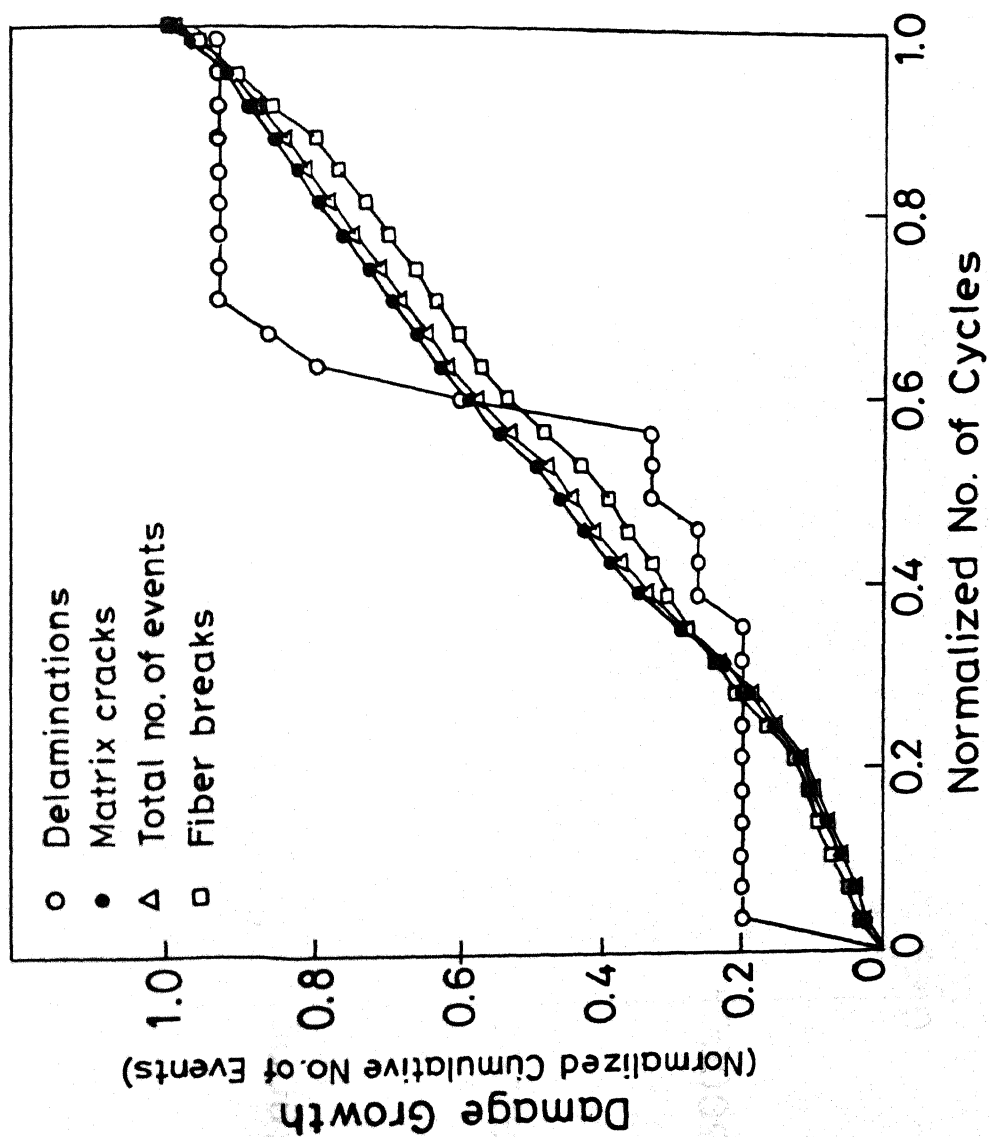
Fig. 4.11 Normalized damage growth in a specimen with
$N_f = 849$.

Legend:
- ○ Delaminations
- ● Matrix cracks
- △ Total no. of events
- □ Fiber breaks

Y-axis: Damage Growth (Normalized Cumulative No. of Events)

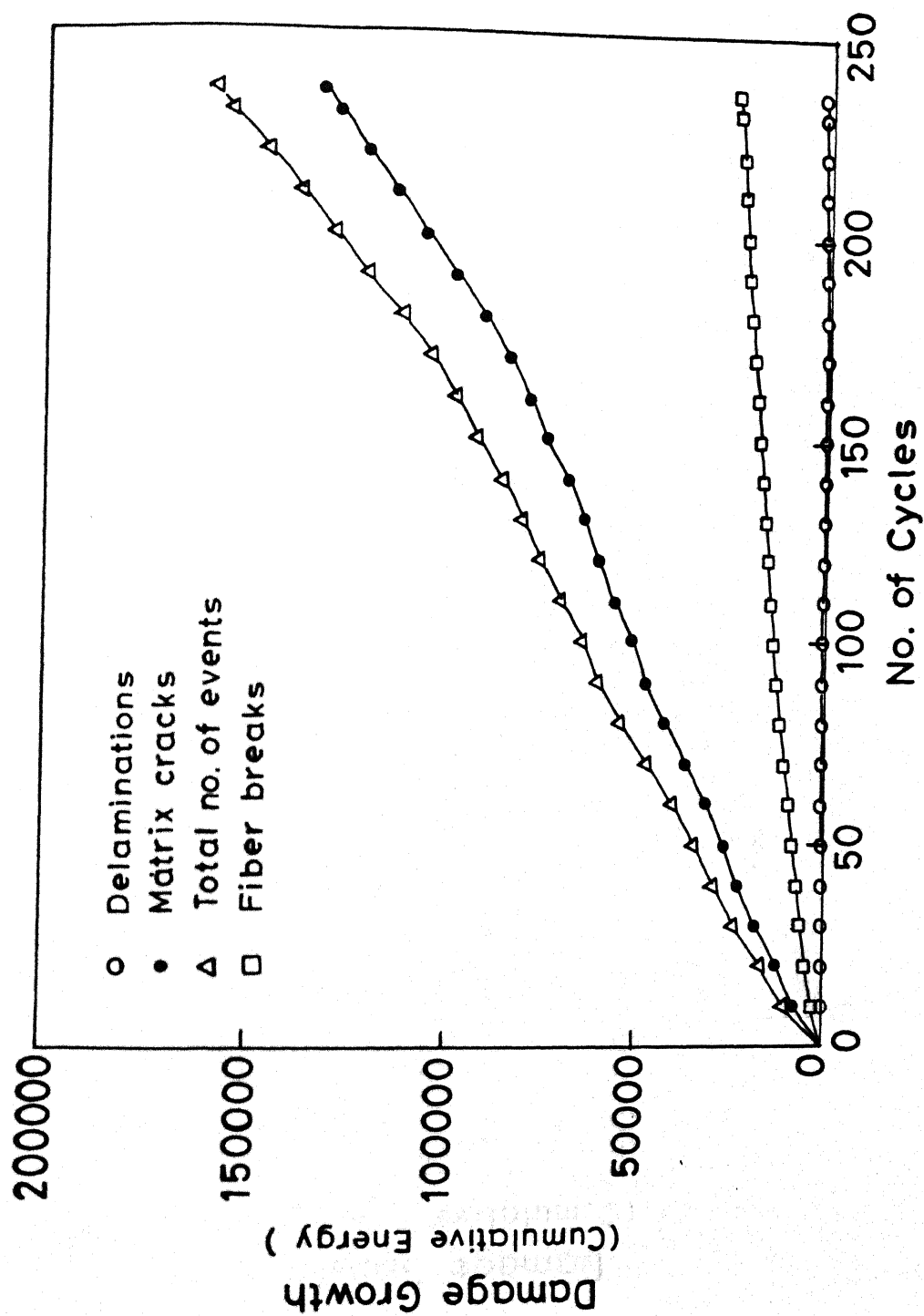X-axis: Normalized No. of Cycles

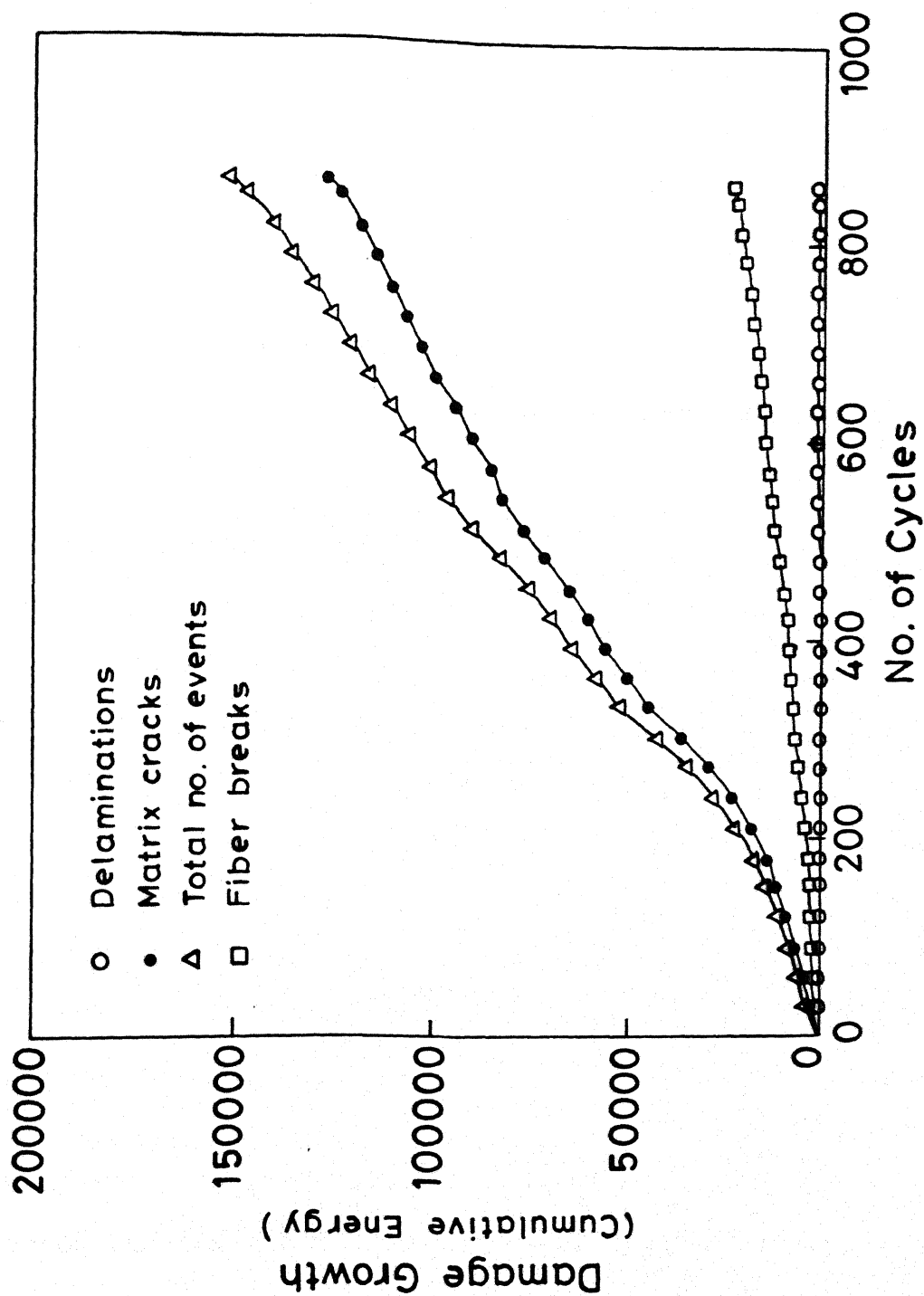Fig.4.12 Damage growth as represented by associated energy released through acoustic emission ($N_f = 237$)

Fig. 4.13 Damage growth as represented by associated energy released through acoustic emission ($N_f = 849$)

Each damage mechanism is expected to influenece the material properties by different amounts. It was assumed that energy associated with each damage event may represent the magnitude of damage severity. Cumulative energy of acoustic emission events has, therefore, been plotted against number of cycles in Figs. 4.12 and 4.13 for the two specimens. These plots are very similar to those shown in Figs. 4.8 and 4.9 but quite different from the one shown in Fig. 4.5. It is therefore, quite clear that neither the number of damage events causing acoustic emissions nor the energy associated with them correlates with the damage indicated by fatigue modulus (Fig. 4.5).

A further attempt has been made to correlate the acoustic emission data with the damage growth as indicated by the change in fatigue modulus (Fig. 4.5). The change in fatigue modulus indicates that during fatigue, damage growth generally occurs in three stages (Section 4.3), although there is no sudden change in damage growth rate at the junction of two stages. Duration or the percent number of cycles in each damage stage depends upon the maximum stress and vary from specimen to specimen. In the present case it was observed that at Smax = 0.9 Su, the three damage stages can generally be considered to occur at 0 to 25, 25 to 96, and 96 to 100 percent of the cyclic life of a specimen. In view of the this observation, the number of different acoustic emission events and their rate of occurence in each of the three damage stages have been obtained (Tables 4.7 and 4.8). The number of events per cycle given in these tables was calculated by considering all the events of one type in a single damage

Table 4.7 No. of damage events for specimen 1

Damage Growth Stage	Number of cycles	No. of events				No. of events/cycle			
		Fiber Break	Matrix crack	Delami nation	Total	Fiber break	Matrix crack	Delami nation	Total
I	4-59	228	527	4	759	4.15	9.58	0.07	13.80
II	60-227	449	1715	14	2178	2.67	10.20	0.08	12.96
III	228-237	33	152	4	189	3.30	15.20	0.40	18.90
Ent.life	237	710	2394	22	3126	2.99	10.10	0.09	13.19

Table 4.8 No. of damage events for specimen 2

Damage Growth Stage	Number of cycles	No. of events				No. of events/cycle			
		Fiber Break	Matrix crack	Delami nation	Total	Fiber break	Matrix crack	Delami nation	Total
I	0-212	99	322	3	424	0.47	1.52	0.01	2.00
II	213-815	438	1702	11	2151	3.57	2.82	0.02	3.56
III	816-849	49	150	1	200	1.44	4.41	0.03	5.88
Ent.life	849	586	274	15	2775	0.69	2.56	0.02	3.27

stage and the total number of cycles in that stage. The number of fibre breaks per cycle does not show a definite trend in damage growth in three stages. Delamination cracks per cycle increase as damage growth changes from stage I to stage II and then from stage II to stage III. However, since the total number of delamination cracks is so small that it is unlikely to account for the loss of fatigue modulus of the specimen particularly since the cumulative energy associated with these cracks is only very small compared to the cumulative energy associated with total acoustic emission events. The number of matrix cracks per cycle also increases as the damage changes from stage I to stage II and then to stage III. The number of matrix cracks per cycle is very large in stage III signifying that matrix cracks play an important role in the final stage of damage growth during fatigue loading. These matrix cracks are probably debonding cracks resulting in the composite acting as a bundle of fibres rather than as the composite material. This may significantly weaken the material and cause its failure.

To study the growth rate of matrix cracks throughout fatigue loading, number of matrix cracks per cycle was calculated for small intervals (20 cycles in one specimen and 50 cycles in the other specimen). The number of matrix cracks per cycle has been plotted against the number of cycles in Figs. 4.14 and 4.15. These plots also indicate that the number of matrix cracks does increase during the final stage of damage growth during fatigue loading.
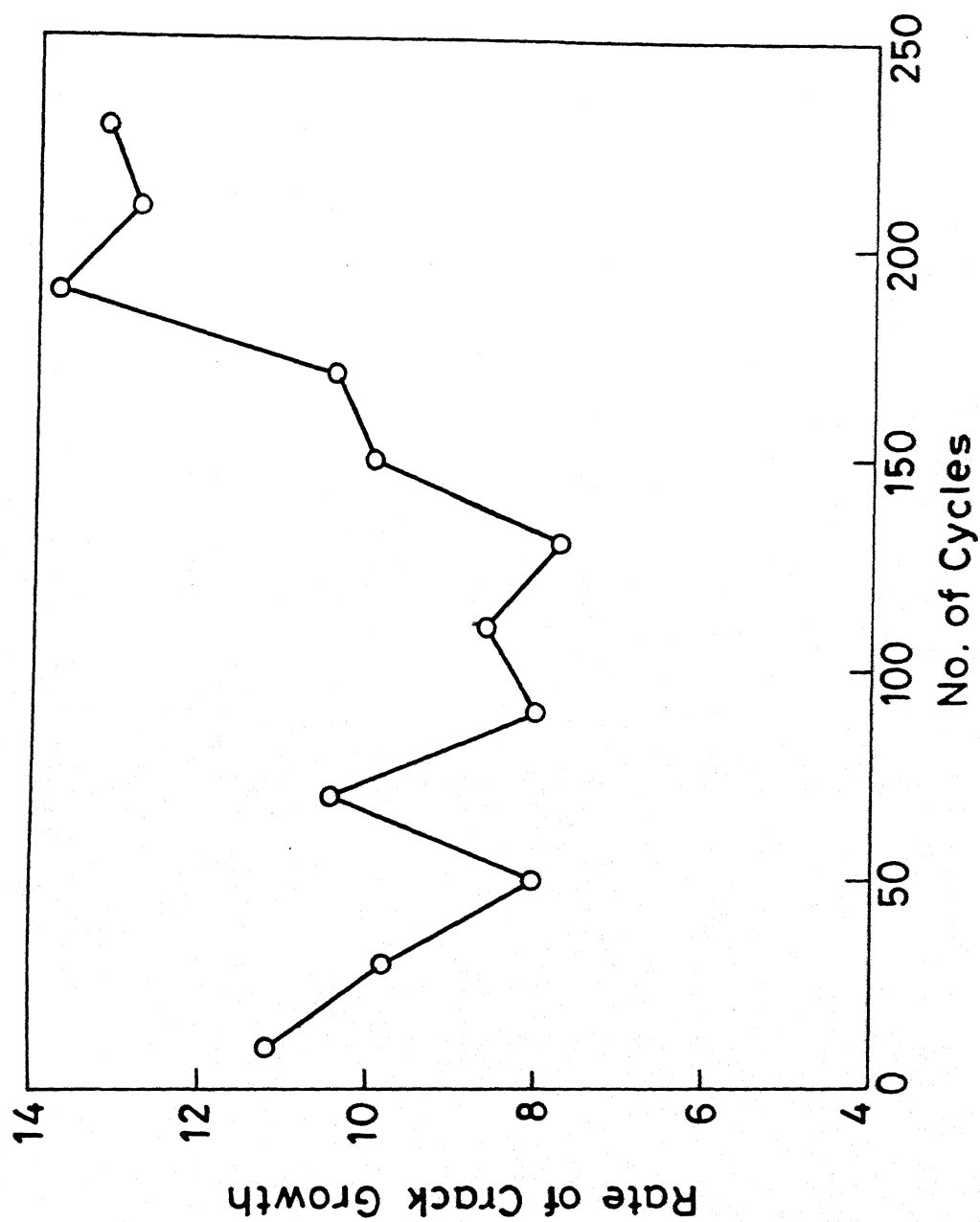
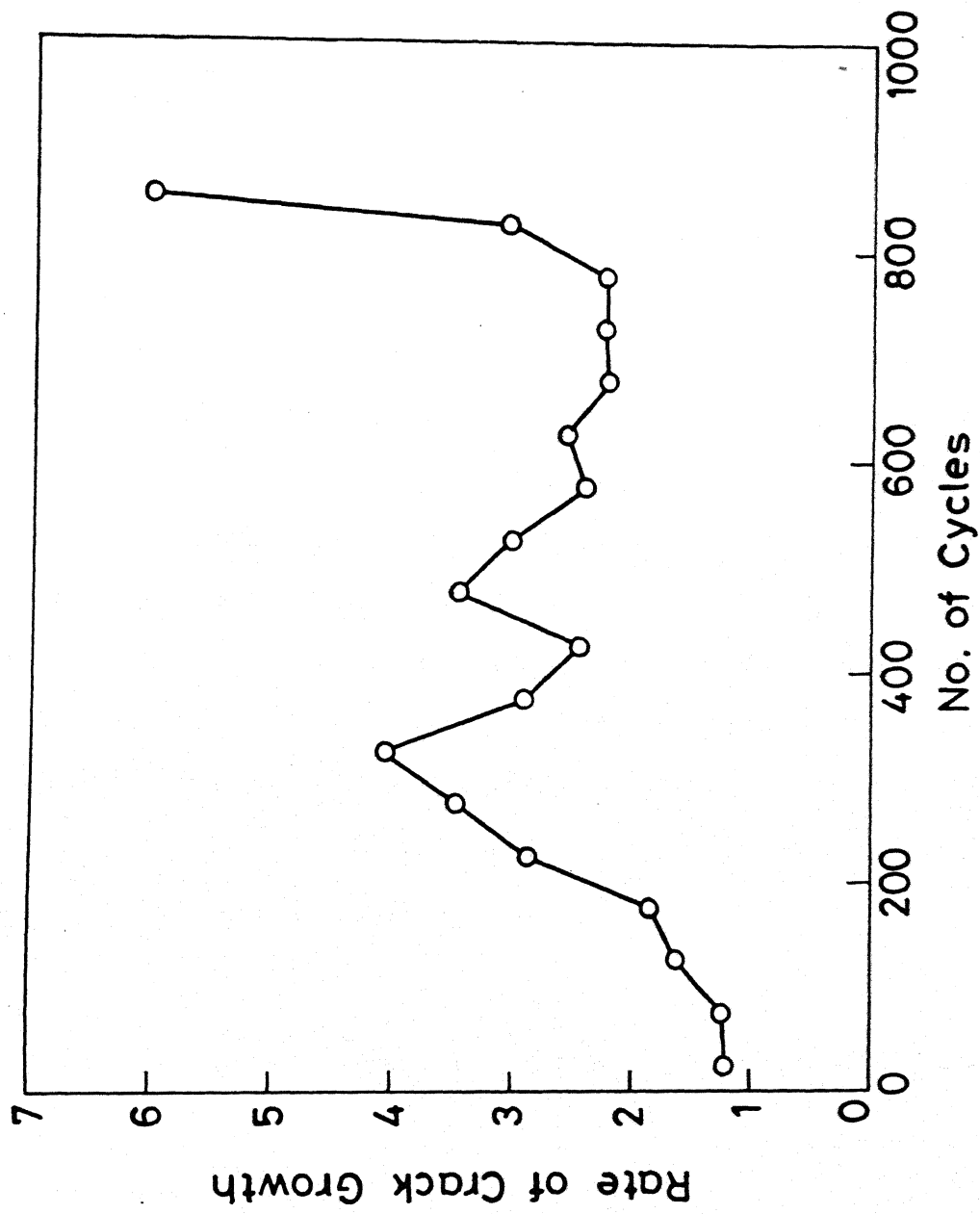Fig.4.14 Rate of crack growth for specimen with $N_f = 237$.

Fig.4.15 Rate of crack growth for specimen with Nf = 849

It may be observed that the total number of acoustic emission events produced in the above two specimens differ by only about 10 % while their cyclic lives are different by a factor of nearly 4. If it is assumed that each event produces an equal amount of damage, the total number of events before failure may be expected to be nearly the same for all specimens irrespective of their fatigue life. However, the other specimens, which showed much larger fatigue life, produced much larger no. of acoustic emission events. This clearly indicates that not all AE events produce equal damage. It has been suggested that many of the acoustic emissions may not emanate from actual material damage but may be caused by fretting or rubbing of the already produced internal surfaces. This actually brings to focus an important limitation of the AE technique to study damage growth, namely, inadequacy of procedure or technique to distinguish the AE events emanating from damage from those emanating from other sources. The present techniques do not provide a solution for the same.

CHAPTER 5

CONCLUSIONS AND SUGGESTIONS FOR FUTURE WORK

5.1 CONCLUSIONS :

From the results obtained during the present work the following conclusions can be drawn :

1. The strain curve during tensile test is linear upto failure for carbon epoxy composite.

2. In carbon epoxy composite, the damage growth occurs in three stages. Beginning of the third stage of damage represents a critical condition beyond which damage grows very fast and failure occurs. The third stage of damage usually spans over last 4 or 5% of total fatigue life.

3. Acoustic emission technique can be employed to study damage in composite materials. As a first step in employing this technique for damage identification and monitoring, acoustic emission characteristics of internal damage mechanisms (that is fibre breaks, matrix cracks, and delamination) have been determined. It is accomplished by conducting tests on specimens in which only one type of damage is predominant in a single test. The results indicate that fibre breaks, matrix cracks, and delamination cracks can be identified on the basis of event duration (ED). An event with ED less than 25 is likely to emanate from a fibre break, with ED between 25 and 200 from a matrix crack, and with ED more than 200 from a delamination crack.

4. To study damage growth during a normal fatigue test, recorded acoustic emission events were first classified into the three

categories representing three damage mechanisms indicated above. The results indicate that neither the number of damage events causing acoustic emissions nor the energy associated with them correlates with the damage indicated by fatigue modulus. It was observed that a sudden increase in the number of matrix cracks per cycle signifies change from second stage of damage to the third stage of damage. These matrix cracks are probably debonding cracks making the composite act like a bundle of fibres rather than a composite material. This will weaken the material significantly and cause its failure. However, further experiments are needed to confirm the trends and make quantitative predictions.

5.2 SUGGESTIONS FOR FUTURE WORK :

1. More controlled experiments should be carried out to determine acoustic emission characteristics of internal damage mechanisms.

2. Experiments should be carried out on specimens with different ply orientations also so that delamination becomes more prominent.

3. New analysis procedures should be developed to identify change in stage of damage particularly change from second stage to third stage.

REFERENCES

1. K.H. Boller, "Fatigue Characteristics of RP Laminates Subjected to Axial Loading", Modern Plastics, Vol. 41, 1964, p. 145.

2. L.J. Broutman and S. Sahu, "Progressive Damage of a Glass Reinforced Plastic During Fatigue", SPI, 24th Annual Technical Conference, Washington D.C., February 1969, Section 11-D.

3. J.W. Dally and B.D. Agarwal, "Low Cycle Fatigue Behaviour of Glass Fibre Reinforced Plastics", Proceedings of the Army Symposium on solid Mechanics, AMMRC MS 70-5, 1970.

4. B.D. Agarwal and L.J. Broutman, "Analysis and Performance of Fiber Composites", John Wiley, New York, 1980.

5. R.F. Dickson et. al., "Effects of Moisture on High Performance Laminates", First International Conference on Acoustic Emission from REinforced Composites, The Society of he Plastics Industry Inc., July 1983, Session 1, p. 1-14.

6. F.J. Guild, M.G. Phillips and B. Harris, "Acoustic Emission From Composites: The Influence of REinforcement Pattern", First International Conference on Acoustic Emission from Reinforced Composites, The Society of the Plastics Industry, Inc. July 1983, Session 3, p. 1-9.

7. F.J. Guild, F.J. Ackerman, M.G. Phillips and B. Harris, "Amplitude Distrubution Analysis of Acoustic Emission from composites: The Development of a Data Collection and Processing System", First International Conference on Acoustic Emission from Reinforced Composites, The society of the Plastics Industry, Inc. July 1983, Session 5, p. 1-7.

8. F.J. Guild, B. Harris and A.J. Willis, "Acoustic Emission from Glass/Polyester Composites: Effect of Fiber Orientation", Journal of Acoustic Emission, Vol. 1, No. 4, 1982, p. 244-250.

9. C.J. Jones et. al., "Environmental Fatigue of Reinforced Plastics", Composites, Vol. 14, No. 3, July 1983, p. 288-293.

10. M.P. Ansell, "Acoustic Emission from Softwoods in Tension", Wood Scie3nce and Technology, Vol. 16, 1982, p. 35-57.

11. P.T. Curtis and B.B. Moore, "A Comparison of the Fatigue Performance of Woven and Non-Woven CFRP Laminates", Proceedings of the ICCM-V, San Diego, 1985, p. 293-314.

12. S. Amijima et. al., "Fatigue Life and Reliability of Satin Woven Glass Cloth FRP under Random Loading", Journal of the Society of Materials Science Japan, Vol. 28, No. 315, 1979, p. 1180-1186.

13. S. Amijima et. al., "A Study on Fatigue Life of FRP Under Random Loading", Journal of the Society of Materials Science Japan, Vol. 30, No. 338, 1981, p. 1123-1128.

14. S. Amijima et. al., "Fatigue Life Estimation of FRP Under Random Loading", Journal of the Society of Materials Science Japan, Vol. 34, No. 378, 1985, p. 293-299.

15. S. Amijima et. al., "Fatigue Crack Propagation Process of Single Edge-Cracked FRP", Journal of The Society of Materials Science Japan, Vol. 34, No. 378, 1985, p. 286-292.

16. S. Amijima et. al. "A Study on the FAtigue Life Estimation of FRP Under Random Loading", Progress in Science and Engineering of Composites, ICCM-IV, Tokyo 1982, p. 701-708.

17. N.G. Ohlson, "Damage in Biaxial Fatigue of Composites", Proceedings of the ICCM-V, San diego, 1985, p. 191-197.

18. M.L. Benzeggagh et. al., "Experimental Analysis of Mode I Delamination Testing", Fifth International Congress on Composite Materials (ICCM-V), W.C. Harrigan, Jr., J. Strife, A.K. Dhingra, Editors, Metallurgical Society, Warrendal, PA, 1985, p. 127-137.

19. David L. Davidson, "A Technique for Microanalysis of Matrix and Fiber-Matrix Interaction During Composite Deformation, Fifth International Congress on Composite Materials (ICCM-V), W.C. Harrigan, Jr., J. Strife, A.K. Dhingra, Editors, Metallurgical Society, Warrendal, PA, 1985, p. 175-189.

20. W.N. Reynolds, "Fatigue Evaluation of Fibre-Reinforced Composite Materials", AERE-R9439, UKAEA, Harwell, April 1979.

21. T.W. Packer and W.N. Reynolds, "Non-destructive Inspection of Glass-Reinforced Plastics", British Journal of NDT, May 1982, p. 135-138.

22. Martine Wevers, "Analysis of Fatigue Damage in CFR Epoxy Composites by Means of Acoustic Emission: Setting Up a Damage Accumulation Theory".

23. B. Echalier and A. Falchi, "Mechanical Behaviour and Acoustic Emission of Glass-Epoxy Wound Structures Under Static and Fatigue Loading", Fifth International Congress on Composite Materials (ICCM-V), W.C. harrigan, Jr., J. Strife, A.K. Dhingra, Editors, Metallurgical Society, Warrendal, PA, 1985, p. 163-173.

24. Michael G. Bader and Lynn Boniface, "Damage Development During Quasi-Static and Cyclic Loading in GRP and CFRP Laminates Containing 90° Plies", Fifth International Congress on Composite Materials (ICCM-V), W.C. Harrigan, Jr., J. Strife, A.K. Dhingra, Editors, Metallurgical Society, WArrendal, PA, 1985, p. 221-232.

25. D. Valentin and A.R. Bunsell, "The Monitoring of Damage Process in CFRP Composite Structures by Amplitude Analysis", Fifth International Congress on Composite Materials (ICCM-V), W.C. Harrigan, Jr., J. Strife, A.K. Dhingra, Editors, Metallurgical Society, WArrendal, PA, 1985, p. 221-232.

26. K.L. Reifsnider, Editor, Damage in Compsoite Materials, ASTM STP 775, American Society for Testing and Materials, 1982.

27. B.D. Agarwal and S.K. Mazumdar, "Damage Initiation and Growth In Kevlar Epoxy Composite Subjected To Axial Fatigue Loading", Journal of The Aero. Soc. of India, Vol.41 No. 4, p. 357-365.

28. Lt. D. Ravi Kumar, " Damage Identification in Kevlar/epoxy composites through cluster analysis of acoustic emission data," M. Tech. Thesis, Dept. of Mech. Engg. I. I. T. Kanpur, Feb. 1989.

29. W. Hwang and K.S. Han, "Fatigue of Composites - Fatigue Modulus Concept and Life Prediction", J. Comp. Mat., Vol. 20, p. 154, March 1986.

30. W. Hwang and K.S. Han, "Cumulative Damage Models and Multi Stress Fatigue Life Prediction", J. Comp. Mat., Vol. 20, p. 125, March 1986.